Chem. Senses 33: 839–859, 2008
doi:10.1093/chemse/bjn048
Advance Access publication August 14, 2008

REVIEW

The Electrochemical Basis of Odor Transduction in Vertebrate Olfactory Cilia

Steven J. Kleene

Department of Cancer and Cell Biology, University of Cincinnati, PO Box 670667, Cincinnati, OH, USA

Correspondence to be sent to: Steven J. Kleene, Department of Cancer and Cell Biology, University of Cincinnati, PO Box 670667, 231 Albert Sabin Way, Cincinnati, OH 45267-0667, USA. e-mail: steve@syrano.acb.uc.edu

Abstract

Most vertebrate olfactory receptor neurons share a common G-protein–coupled pathway for transducing the binding of odorant into depolarization. The depolarization involves 2 currents: an influx of cations (including Ca^{2+}) through cyclic nucleotide-gated channels and a secondary efflux of Cl^- through Ca^{2+}-gated Cl^- channels. The relation between stimulus strength and receptor current shows positive cooperativity that is attributed to the channel properties. This cooperativity amplifies the responses to sufficiently strong stimuli but reduces sensitivity and dynamic range. The odor response is transient, and prolonged or repeated stimulation causes adaptation and desensitization. At least 10 mechanisms may contribute to termination of the response; several of these result from an increase in intraciliary Ca^{2+}. It is not known to what extent regulation of ionic concentrations in the cilium depends on the dendrite and soma. Although many of the major mechanisms have been identified, odor transduction is not well understood at a quantitative level.

Key words: adaptation, chloride channels, cyclic-nucleotide-gated channels, desensitization, olfaction

Introduction

Vertebrate olfactory receptor neurons (ORNs) transduce binding of odorant molecules into an electrical response that can ultimately lead to the generation of action potentials (APs). Beginning with the discovery of an olfactory adenylyl cyclase (Pace et al. 1985), it has become clear that the majority of vertebrate ORNs achieve odor transduction through a G-protein–coupled cascade that uses cyclic adenosine 3′:5′-monophosphate (cAMP) and Ca^{2+} as second messengers. What follows is a review of our current knowledge of that cascade, with an emphasis on the electrical events and ion channels that reside in the olfactory cilia. To the extent possible, I will focus on how transduction is believed to operate in vivo. For topics not addressed here (stimulus quality coding and discrimination, alternate transduction mechanisms, channel structures, voltage-gated channels, and development), other reviews may be consulted (Schild and Restrepo 1998; Firestein 2001; Kaupp and Seifert 2002; Touhara 2002, 2007; Matthews and Reisert 2003; Bradley et al. 2005; Ache and Young 2005; Rawson and Yee 2006; Mori et al. 2006; Pifferi, Boccaccio, and Menini 2006; Malnic 2007; Elsaesser and Paysan 2007; Ma 2007).

The primary ORN

Odorants are detected at the surface of the olfactory epithelium, which lines parts of the nasal cavity. The epithelium contains several cell types (Figure 1A; see Menco and Morrison [2003] for additional details). The basal progenitor cells may differentiate into supporting (sustentacular) cells or into ORNs. The supporting cells and glandular cells secrete a mucus layer that coats the luminal surface of the epithelium. The primary receptor neurons are bipolar (Figure 1B). One process of each neuron is a single, unbranched axon that synapses in the olfactory bulb of the brain. On sufficient depolarization, the neuron can generate one or more APs. The second process of each neuron is a dendrite that projects into the mucus and terminates in an olfactory knob or vesicle. From each knob, fine olfactory cilia emanate into the mucus.

Long before any of the molecular components were identified, evidence suggested that olfactory transduction takes place in the neuronal cilia (Adamek et al. 1984; Getchell 1986). The ORNs of lower vertebrates typically have about 6 motile cilia that can be as long as 200 μm (Hopkins 1926; Reese 1965; Menco 1980). The diameter of the cilium tapers, in frog from 0.28 μm near the base of the cilium to 0.19 μm in

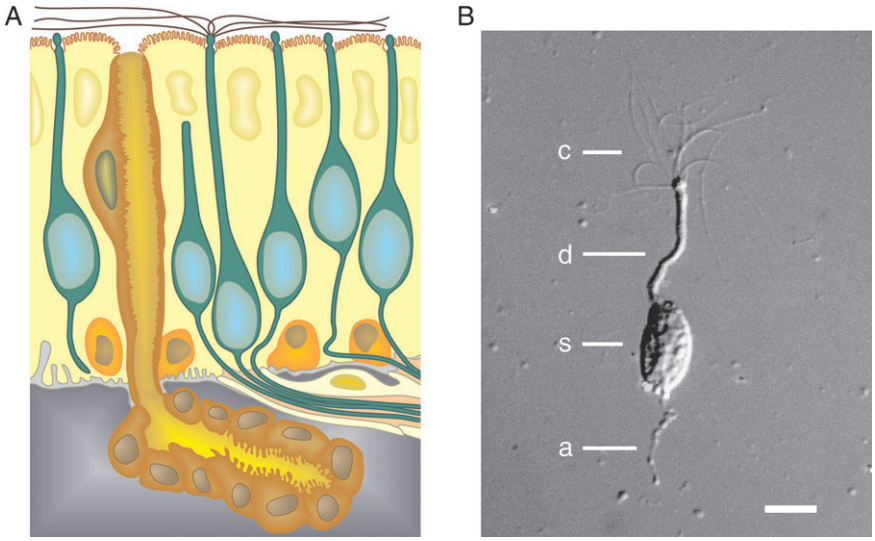

Figure 1 **(A)** Schematic of vertebrate olfactory epithelium. ORNs are shown in green. Each ORN projects a dendrite to the apical (luminal) surface of the epithelium (top of the figure). This surface is covered with mucus (not shown) that surrounds the dendritic knobs and olfactory cilia. For clarity, the cilia of just one ORN are shown. The ORN that has not reached the apical surface is immature. The mucus is formed by secretions of the supporting (sustentacular) cells (shown in yellow) and the Bowman's glands (shown projecting a duct through the epithelium). Basal progenitor cells are shown in orange at the base of the epithelium. **(B)** Photograph of an isolated frog ORN under differential interference contrast optics. c, cilia; d, dendrite; s, soma; a, axonal segment. The calibration bar represents 10 μm. Reprinted from Kleene and Gesteland (1981), copyright 1981, with permission from Elsevier.

the distal portion (Menco 1980). In mammals, the cilia are shorter (15–50 μm), thinner (tapering to 0.11 μm), more numerous (averaging 17 per neuron), and nonmotile (Menco 1980; Lidow and Menco 1984; Menco and Morrison 2003). In all cases, the cilia provide a considerable surface area with which an odorant molecule might collide.

The extracellular environment of the ORN is not well characterized but certainly includes multiple compartments. The cilia and most olfactory knobs reside in the mucus, and the proximal and distal segments of the cilia reside within different mucous domains (Menco and Farbman 1992). The dendrite (below the knob), soma, and axon are exposed to fluids of unknown composition.

Methods of electrical recording

The electrical properties of ORNs will be reviewed in detail. Before assessing any of the experimental results, it is important to appreciate the strengths and limitations of the many electrical recording methods that have been used.

Ottoson (1956) was the first to measure an odor-induced electrical activity in olfactory epithelium. On presentation of an odorous vapor, Ottoson recorded a potential difference between the surface of the epithelium and a reference electrode. This "electroolfactogram" (EOG) arises from the summated receptor potentials of many ORNs in the region (Ottoson 1956; Scott and Scott-Johnson 2002). It does not allow the study of individual ORNs.

By penetrating the epithelial surface with a metal-filled microelectrode, Gesteland et al. (1965) was able to record extracellularly the excitation or inhibition of individual ORNs by odors (see also Sicard and Holley 1984; Kang and Caprio 1995; Duchamp-Viret et al. 2000). Later, sharp electrodes were used to record intracellularly from single ORNs in situ (Getchell 1977; Trotier and MacLeod 1983).

All the work described so far was done in live, anesthetized animals. As a result, the epithelium was intact, and each ORN was in its native environment. It is also possible to record from neurons in an intact epithelium after the epithelium is surgically removed. Such removal allows EOG recording while flowing liquid-phase stimuli over the tissue (Chen et al. 2000; Nickell et al. 2007). Drawing olfactory cilia into a pipette at the epithelial surface allows recording of neuronal APs (Frings and Lindemann 1991). Ma and coworkers have been able to record from single ORNs in intact epithelium using the perforated patch method (Ma et al. 1999; Grosmaitre et al. 2006). This method allows voltage and current clamping while leaving the neuronal membrane and environment intact.

The remaining methods proceed after dissociation of the epithelium. In a few cases, neurons have been patch clamped in slices of epithelial tissue (Firestein and Werblin 1989; Trotier 1994; Tomaru and Kurahashi 2005). However, most of what we know of olfactory transduction has been from studies of individual ORNs dissociated from the epithelium. The several natural extracellular compartments are replaced by a single saline that is hoped to be physiological, and any modulators present in the mucus are lost. The benefit, of course, is that the extracellular and cytoplasmic constituents may be varied at will. Intact ORNs may be recorded under patch clamp while attached to the recording pipette by the soma or dendrite (Maue and Dionne 1987; Lynch and Barry

1989; Chiu et al. 1997) or by a single cilium (Kleene and Gesteland 1991a; Delgado and Bacigalupo 2004). The perforated patch method has also been applied (Kurahashi and Yau 1993; Trotier 1994; Zhainazarov and Ache 1995). Most often, though, the patch is ruptured to yield the whole-cell recording configuration (Trotier 1986; Anderson and Hamilton 1987; Firestein and Werblin 1987; Firestein et al. 1990; Kurahashi 1990). The cytoplasm is gradually diluted by the pipette solution, and the response to odors may decay over periods as short as 5–15 min (Trotier 1986; Frings and Lindemann 1988). The vast majority of these studies have used voltage clamp rather than current clamp.

By some criteria, the most successful method for recording from intact, single ORNs has been the loose-patch (suction pipette) method (Lowe and Gold 1991; Trotier 1994; Reisert and Matthews 1999). The entire apical or basal end of a neuron is pulled into a recording pipette, and the membrane is left intact. The odor response can survive for at least 190 repeated stimulations over a period of hours (Bhandawat et al. 2005). Voltage cannot be clamped or current injected. This limits experimental control but also more closely reflects the natural state.

Even the least natural recording situations have contributed greatly to our understanding of olfactory transduction. Membrane patches can be excised from the dendrite or soma (Zufall and Firestein 1993; Kurahashi and Kaneko 1993) or even from the cilia themselves (Nakamura and Gold 1987; Kurahashi and Kaneko 1993; Delgado et al. 2003). It is also possible to excise a single intact cilium for recording (Kleene and Gesteland 1991a). These methods have proven useful for characterizing the transduction channels, but it has not yet been possible to demonstrate the full odor transduction cascade in an excised patch.

Although not strictly an electrical recording method, imaging of ion-sensitive fluorescent indicators has also enhanced our understanding of the roles of Ca^{2+} (Restrepo et al. 1990; Hirono et al. 1992; Leinders-Zufall et al. 1997, 1998; Reisert and Matthews 2001c; Omura et al. 2003) and Cl^- (Kaneko et al. 2004) in transduction.

Choice of stimulus

To no one's surprise, demonstrating an odor response in a single ORN is difficult. A given neuron responds to a small and unpredictable subset of the many available odorants, so many presentations are ineffective. To increase the likelihood of a response, it is common to present odorants at concentrations ranging from 1 μM to 10 mM. Another strategy is to apply a mixture of several odorants with the hope that one will be appropriate for the chosen ORN. Cineole, *n*-amyl acetate, and isoamyl acetate are often used with success.

When an effective ligand can be predicted, the response rate is very high. Of those ORNs in intact mouse epithelium expressing the MOR23 odorant receptor, 100% responded to lyral, a known MOR23 ligand (Grosmaitre et al. 2006). Even among isolated ORNs from rat, every neuron tested that was found to express the I7 receptor responded to *n*-octanal (Zhao et al. 1998). However, in a mouse engineered to express that same receptor in every mature ORN, only 20% of the ORNs responded to an appropriate ligand (Reisert et al. 2005). One can imagine that many cilia break off during dissociation. However, 94% of murine ORNs respond when cAMP is released inside the neuron (Lagostena and Menini 2003). Because most of the cAMP-gated channels are on the cilia, this suggests that the cilia remain after isolation of the neurons.

Most often, an effective stimulus must be found by trial and error. In this case, anywhere from 2% to 30% of isolated amphibian ORNs respond, depending on the choice of odorant (Kurahashi 1989; Takeuchi et al. 2003; Takeuchi and Kurahashi 2003, 2005). Success rates are lower in mouse, typically ranging from 3% to 12% (Lagostena and Menini 2003; Oka et al. 2004; Reisert et al. 2007). Some evidence suggests that more neurons respond to odors when the epithelium is intact. In frog, rat, and catfish, several odorants elicited responses in 30–80% of single ORNs in situ (Sicard and Holley 1984; Kang and Caprio 1995; Duchamp-Viret et al. 2000).

Certain pharmacological agents increase cytoplasmic cAMP and activate the later stages of the transduction cascade. Forskolin stimulates the adenylyl cyclase, and the cAMP produced activates a neuronal current (Frings and Lindemann 1991). A similar current is produced by stimulation with 3-isobutyl-1-methylxanthine (IBMX), a phosphodiesterase inhibitor that reduces the hydrolysis of cAMP produced by the cell (Frings and Lindemann 1991; Firestein, Darrow, and Shepherd 1991; Firestein, Zufall, and Shepherd 1991; Lowe and Gold 1993b). Membrane-permeant analogues of cAMP can be applied extracellularly (Frings and Lindemann 1991; Firestein, Darrow, and Shepherd 1991), and cAMP itself can be introduced through the recording pipette (Kurahashi 1990). Finally, photocaged cAMP (Lowe and Gold 1993a, 1993b; Kurahashi and Menini 1997; Takeuchi and Kurahashi 2002, 2005, 2008) and Ca^{2+} (Boccaccio and Menini 2007) may be introduced through the pipette and released by photolysis to generate the cytoplasmic second messengers.

An extraordinary amount has been learned by studying isolated cells and cell membranes, stimulating with high concentrations of odorants, and applying voltage clamp. Still, it should be appreciated that an ability to record under more physiological conditions could turn up some surprises.

Electrical response to odors in single ORNs

In isolated ORNs, the response to odorous stimuli in solution has been well characterized. This section describes the principal features of that response.

Most often, the response has been measured under voltage clamp on presentation of a brief pulse of odorant. Of the

neurons that respond, most (but not all) generate a transient inward receptor current (Figure 2A) that would be expected to depolarize the neuron in situ. The response typically lasts 1 s or more. In amphibians, the latency between arrival of the stimulus and the onset of the current ranges from 150 to 600 ms (Firestein and Werblin 1987; Kurahashi 1989; Firestein et al. 1990; Takeuchi et al. 2003; Tomaru and Kurahashi 2005). In mouse and rat, the latency is at most 160 ms (Reisert and Matthews 2001a; Grosmaitre et al. 2006). This shorter latency is observed even in intact epithelium, which requires that the odorant diffuse through the mucus (Grosmaitre et al. 2006). For a strong stimulus, the amplitude of the peak receptor current can be several hundred pA (e.g., 700 pA in salamander [Firestein et al. 1990]; 950 pA [Lowe and Gold 1993b] to 1.5 nA in rat [Ma et al. 1999]). By directing the stimulus to various parts of the cell, it has been shown that the sensitivity to odorants is largely restricted to the cilia (Kurahashi 1989; Firestein et al. 1990; Lowe and Gold 1991; Takeuchi et al. 2003).

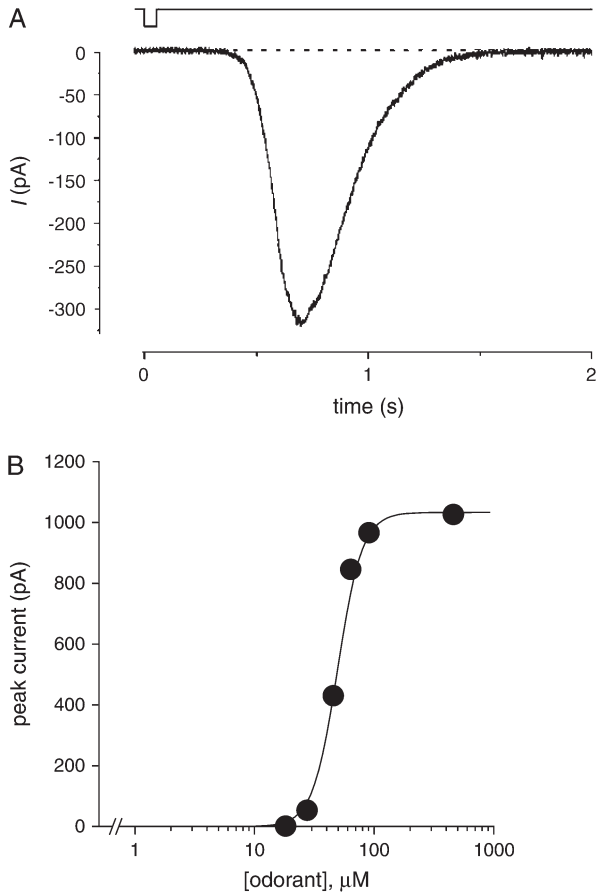

Figure 2 Electrical response to odorants in isolated ORNs voltage clamped under whole-cell recording. **(A)** Response of an ORN from newt to the odorant lilial at a holding potential of −54 mV. The square pulse in the top trace represents the 100-ms presentation of lilial. Modified from Takeuchi et al. 2003 (*The Journal of General Physiology*, 122:255–264, copyright 2003, The Rockefeller University Press). **(B)** Response of a salamander ORN to the odorant isoamyl acetate as a function of odorant concentration. At each of 6 concentrations, a 1.2-s pulse of odorant was presented, and the peak amplitude of the receptor current was measured. The solid line is the best-fitting Hill function, which has the parameters I_{max} = 1034 pA, $K_{½}$ = 53 μM, and n = 4.2. Holding potential −55 mV. Currents in (B) are inward but assigned positive values. Reprinted from Firestein et al. (1993) with permission from Blackwell Publishing.

During the odor response, cytoplasmic Ca^{2+} increases transiently (Restrepo et al. 1990; Hirono et al. 1992; Leinders-Zufall et al. 1997, 1998; Reisert and Matthews 2001c; Omura et al. 2003) with a time course that parallels that of the odor-induced current (Leinders-Zufall et al. 1997; Reisert and Matthews 2001c). The Ca^{2+} increase is first seen in the cilia, and the Ca^{2+} signal decays faster in the cilia than in the dendrite or soma (Leinders-Zufall et al. 1997, 1998).

For stimuli of moderate strength, the neuronal response represents an integral of the stimulus over time. Thus, the amplitude of the peak of the receptor current can be increased by increasing either the concentration or the duration of the stimulus pulse (Firestein et al. 1993; Takeuchi and Kurahashi 2002). An example of the relation between odorant dose and peak receptor current is shown in Figure 2B. The relation is well fit by a Hill function:

$$I = I_{\max}\frac{c^n}{c^n + K_{½}^n},$$

where I_{max} is the maximum macroscopic current, c is the concentration of odorant, $K_{½}$ is the half-maximally effective concentration, and n is the Hill coefficient. In isolated salamander ORNs under whole-cell recording, $K_{½}$ for the 3 odorants tested ranged from 3 to 90 μM (Firestein et al. 1993). A similar range (4–104 μM) was observed when mouse ORNs were studied under more physiological conditions (Grosmaitre et al. 2006). However, some neurons in that study responded to as little as 10 nM of the odorant lyral. In frog, some ORNs in intact epithelium responded to just 1 pM cineole (Frings and Lindemann 1990).

The other Hill parameter, n, describes the slope of the rising phase of the dose–response relation. In Figure 2B, n = 4.2, and the receptor current increases over about a 10-fold range of odorant concentration (Firestein et al. 1993). As n decreases, the slope also decreases, causing an increase in the range of stimulus strengths over which the neuronal response varies (dynamic range). In isolated amphibian ORNs under whole-cell recording, n ranges from 2.7 to 9.7 (Firestein et al. 1993; Tomaru and Kurahashi 2005; Takeuchi and Kurahashi 2005). When recordings are made without disrupting the neuronal membrane, n is much smaller (0.8–1.8; frog [Reisert and Matthews 1999], mouse [Grosmaitre et al. 2006], and rat [Ma et al. 1999]), and the neurons respond over as much as a 1000-fold range of odorant concentration. For a given odorant, the dose–response relation varies considerably from one neuron to the next (Firestein et al. 1993; Tomaru and Kurahashi 2005), even among neurons known to express the same odorant receptor (Grosmaitre et al. 2006). The relation between odorant

dose and frequency of APs in ORNs is similar to that for the receptor current. However, the relation for APs is shifted to somewhat lower odorant concentrations (Reisert and Matthews 1999; Tomaru and Kurahashi 2005). In physiological solutions, the current-voltage relation of the odor-induced current is nearly linear with slight outward rectification (Kurahashi 1989; Kurahashi and Shibuya 1990; Takeuchi and Kurahashi 2003). The reversal potential ranges from 0 to +2.8 mV (Lowe and Gold 1993a; Takeuchi et al. 2003; Takeuchi and Kurahashi 2003).

Adaptation and desensitization

With prolonged or repeated odor stimulation, the ORN shows a property variously described as adaptation, desensitization, or inactivation. Two experimental approaches have been used to demonstrate this. In the first, a prolonged odor stimulus is applied. Despite the continued presence of the stimulus, the receptor current decreases with time (Figure 3A, recording at the left; Kurahashi and Shibuya 1990; Firestein et al. 1990; Zufall, Shepherd, and Firestein 1991; Reisert and Matthews 1999). A similar result ensues if cAMP is allowed to diffuse into the cell via the patch pipette (Kurahashi 1990). In either case, the decrease in current can be largely eliminated if Ca^{2+} is removed from the extracellular bath (Figure 3A, recording at the right; Kurahashi and Shibuya 1990; Kurahashi 1990; Zufall, Shepherd, and Firestein 1991). When guanosine 3′:5′-cyclic monophosphate (cGMP) is produced by photolysis of caged cGMP over a prolonged period in a mouse ORN, the receptor current decreases with time (Lagostena and Menini 2003). Curiously, the receptor current shows little decrease during photolysis of caged cAMP in ORNs from newt (Takeuchi and Kurahashi 2002). The reason for this discrepancy is not understood.

Adaptation can also be demonstrated by delivering a pair of identical, brief stimulus pulses in succession (Figure 3B). The stimulus may be an odorant or cAMP produced by photolysis. If the interval between the pulses is sufficiently short, the amplitude of the second pulse is reduced (Figure 3B, recording at the left). At that point, the cell is in an adapted state, the first (conditioning) pulse having desensitized the neuron to subsequent stimuli. The desensitization is greater with shorter interstimulus intervals (Kurahashi and Shibuya 1990; Kurahashi and Menini 1997; Takeuchi et al. 2003). The desensitization disappears gradually and is not observed when the interval between pulses is sufficiently long (Figure 3B, recording at the right).

Adaptation both shifts and broadens the dynamic range of the neuron (Figure 3C; Kurahashi and Menini 1997; Reisert and Matthews 1999; Boccaccio et al. 2006). In the adapted state, a stronger stimulus is required to produce a half-maximal response. The slope of the dose–response curve is also reduced, indicating that the neuronal response is graded with stimulus strength over a greater range of concentrations. During a prolonged exposure to an odorant, adaptation is expected to continuously reset the neuron to discriminate higher odorant concentrations without saturating. Whether adaptation diminishes the maximum amplitude of the receptor current appears to depend on the experimental protocol. With brief repeated pulses of cytoplasmic cAMP, the maximum amplitude decreases very little (Figure 3C; Kurahashi and Menini 1997; Boccaccio et al. 2006; Song et al. 2008). During prolonged stimulation with strong odor stimuli, though, the maximum amplitude probably decreases (Reisert and Matthews 1999).

A minority of studies have been conducted using methods that allow the neuronal voltage to vary (extracellular, current-clamp, or suction-pipette recording). Under current clamp, the response to a brief stimulus typically consists of a slow depolarization and one or more APs (Getchell 1977; Kurahashi 1989; Firestein et al. 1990; Grosmaitre et al. 2006). However, prolonged stimulation often evokes a regular oscillation of the extracellular potential (current clamp; Frings and Lindemann 1988) or current (suction pipette; Reisert and Matthews 2001a, 2001b, 2001c). The oscillations are slow, with periods ranging from 3.5 to 12 s (Reisert and Matthews 2001b). During each cycle of depolarization, intraciliary Ca^{2+} increases (Reisert and Matthews 2001c). Bursts of APs may also occur at each peak of depolarization.

Generation of the receptor current—an overview

Most vertebrate ORNs share a common pathway for generation of the odor-induced receptor current. The major elements of that pathway are now well established (Figure 4), and all of them occur in the membrane of the olfactory cilium (reviewed in Menco and Morrison 2003). Transduction is initiated when an odorant in the mucus binds to an odorant receptor protein (Buck and Axel 1991; Touhara 2002, 2007; Malnic 2007). The activated receptor can then activate G_{olf}, a guanosine triphosphate (GTP)-binding protein (Jones and Reed 1989). G_{olf} in turn activates a type III adenylyl cyclase (Bakalyar and Reed 1990), which increases the concentration of cAMP within the ciliary lumen. A sufficient concentration of cAMP can then gate the first of 2 transduction channels: a cyclic nucleotide-gated (CNG) channel (Nakamura and Gold 1987; Dhallan et al. 1990). The CNG channels conduct a depolarizing inward current of cations, including Ca^{2+}, into the cilium. If sufficient Ca^{2+} accumulates inside the cilium, it gates the second transduction channel: a Ca^{2+}-gated Cl^- channel (Kleene and Gesteland 1991b; Kurahashi and Yau 1993; Kleene 1993b; Lowe and Gold 1993b; Reisert et al. 2003). This channel allows an efflux of Cl^- (i.e., an inward current) that further depolarizes the neuron.

Sections to follow will explain how the properties of the 2 types of transduction channel shape the generation of the receptor current as well as its termination and adaptation.

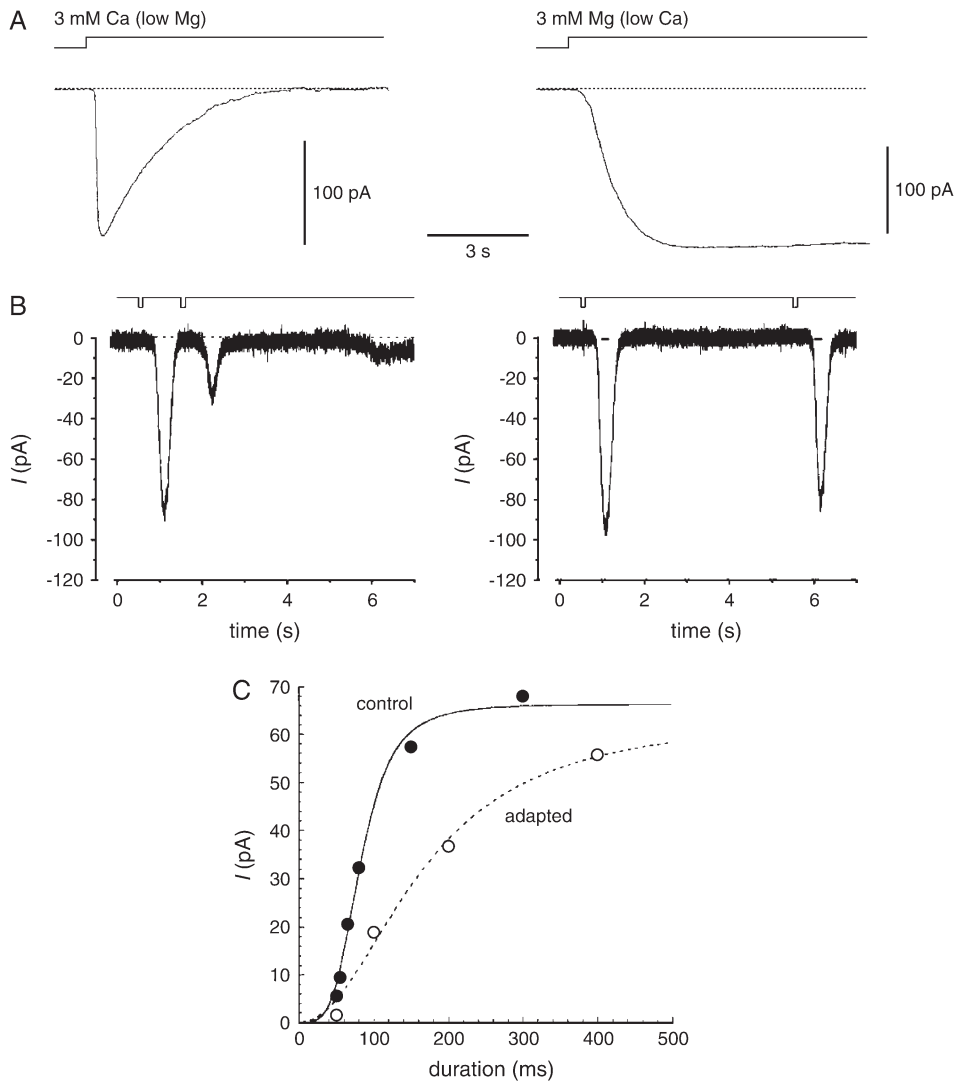

Figure 3 Adaptation and desensitization in isolated newt ORNs voltage clamped under whole-cell recording. **(A)** Desensitization during prolonged odor stimulation. In each recording, the bar at the top represents a prolonged stimulation with 10 mM *n*-amyl acetate. The left recording was made in the presence of 3 mM extracellular Ca^{2+}; the response was transient. When the Ca^{2+} was replaced with 3 mM Mg^{2+} (recording at the right), the response did not appreciably decay. Holding potential −34 mV. Reprinted from Kurahashi and Shibuya (1990), copyright 1990, with permission from Elsevier. **(B)** Desensitization during repeated odor stimulation. In each recording, the top trace indicates 2 identical 100-ms pulses of the odorant lilial (1 mM) delivered with an interval in between. When the interval was 1 s (recording at the left), the response to the second pulse was reduced by 67%. With a 5-s interval (recording at the right), the response was reduced by just 15%. Holding potential −54 mV. Modified from Takeuchi et al. 2003 (*The Journal of General Physiology*, 122:255–264, copyright 2003, The Rockefeller University Press). **(C)** Adaptation increases the dynamic range of the odor response. The solid circles (control) show the dose–response relation for the odorant amyl acetate when odor pulses were presented far enough apart that no desensitization occurred. Stimulus intensity is represented on the *x* axis as the duration of the pulse. The best-fit Hill equation (solid line) has parameters I_{max} = 66 pA, $K_{½}$ = 82 ms, and n = 3.9. The open circles show the dose–response relation when the test pulse was delivered 2.5 s after a conditioning pulse that caused desensitization. The best-fit Hill equation (solid line) has parameters I_{max} = 64 pA, $K_{½}$ = 167 ms, and n = 2.1. Holding potential −50 mV. Currents in (C) are inward but assigned positive values. Reprinted by permission from Macmillan Publishers Ltd (*Nature*, Kurahashi and Menini [1997]), copyright 1997.

First, though, it is worth considering the resting electrical properties of the ORN. These properties are expected to profoundly influence the odor response.

Resting electrical state of the ORN

In the whole-cell configuration, a wide range of input resistances (0.4–30 GΩ) has been measured for the ORN. The input resistance is the sum of 2 resistances in parallel: that of the membrane and that of a shunt between the membrane and the recording pipette (Lynch and Barry 1991; Kawai et al. 1996; Pun and Kleene 2004). In frog ORNs, the true membrane resistance after correcting for the shunt was estimated to be 4–6 GΩ (Pun and Kleene 2004). In such a neuron, a receptor current of just 1 pA should depolarize the cell by 5 mV. It is likely that the smaller mammalian neurons have

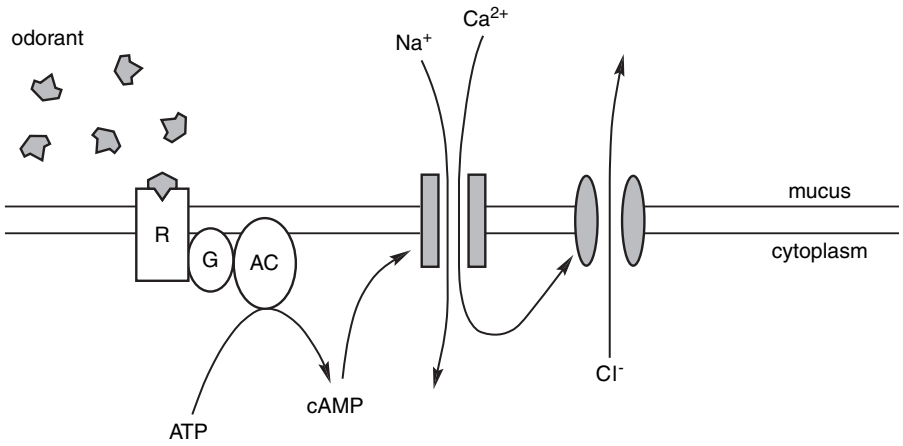

Figure 4 Cascade for generation of the olfactory receptor current in vertebrates. The parallel horizontal lines represent the inner and outer faces of the cytoplasmic membrane of one cilium of an ORN. R, odorant receptor protein; G, G_{olf}, a GTP-binding protein; AC, type III adenylyl cyclase; shaded rectangles, a CNG cationic channel; shaded ellipses, a Ca^{2+}-gated Cl^- channel. Modified from Kleene (2002), copyright 2002, with permission from Elsevier.

higher resistances. The average resting resistance of rat ORNs was estimated to be 26 GΩ (Lynch and Barry 1991).

At initiation of a receptor response, the amplitudes and directions of the ionic fluxes will be determined by the electrochemical driving forces on each ion at rest. These in turn depend on the resting membrane potential and on the concentration gradient of each ion across the membrane. Estimates of the resting membrane potential range from –30 to –90 mV (reviewed by Lagostena and Menini 2003). After correction for the shunt, it was found that the resting potential of a frog ORN is no more negative than –75 mV (Pun and Kleene 2004). This value is set by the ionic selectivity of any conductances that are active at rest. In frog, the membrane at rest conducts K^+ and, to a lesser extent, Na^+ and Ca^{2+} (Kleene 1993b; Pun and Kleene 2004). There is little or no resting Cl^- conductance in ORNs from rat (Okada et al. 2000) or frog (Pun and Kleene 2004). It is not known which cellular compartments control the resting membrane potential. The neuronal membrane contacts at least 3 extracellular environments: the mucus, an interstitial fluid, and a basolateral fluid. For the most part, the ionic compositions of these, and of the cytoplasm, have not been studied.

The resting resistance of the cilium itself should influence both generation and conduction of the receptor potential. Measurements in intact cells indicated a small ciliary permeability to K^+ (Firestein et al. 1990; Lowe and Gold 1991). In isolated frog cilia, the membrane was found to conduct K^+ and, to a lesser extent, Na^+ and Ca^{2+} (Kleene 1992, 1993b). No resting ciliary Cl^- conductance was detectable. Part of the ciliary cationic conductance is attributable to spontaneous gating of the CNG channels (Kleene 2000).

As transduction begins, the driving force on each ion will be determined in part by the ion's concentration gradient across the apical membrane. Table 1 shows estimates of the concentration gradients for the principal ions at the dendritic knob or cilium. Two features are immediately obvious:

Table 1 Resting electrochemical gradients at the apical end of the ORN

Ion or transporter	$[ion]_{in}$ (mM)	$[ion]_{out}$ (mM)	E_{rev} (mV)	Predicted fluxes at −75 mV
Na^+	53 ± 31	55 ± 12	+1	Na^+ in
K^+	172 ± 23	69 ± 10	−24	K^+ in
Free Ca^{2+}	0.000040 ± 0.000009	4.8	+156	Ca^{2+} in
Cl^-	54 ± 4	55 ± 11	0	Cl^- out
NKCC			—	Na^+,K^+,Cl^- out
KCC			—	K^+,Cl^- out
NCX			−310	Na^+ out, Ca^{2+} in

Most of the ionic concentrations shown were measured by energy-dispersive X-ray microanalysis in dendritic knobs of rat ORNs (Reuter et al. 1998). Those values represent total rather than free ionic concentrations. Three of the concentrations were measured by other methods, as follows. $[Ca^{2+}]_{in}$ was measured in salamander cilia with a Ca^{2+}-sensitive fluorescent dye (Leinders-Zufall et al. 1997). $[Ca^{2+}]_{out}$ was determined with a Ca^{2+}-sensitive microelectrode in olfactory mucus of rat (Crumling and Gold 1998); the value shown is the midpoint of the range reported (2.6–7.1 mM). $[Cl^-]_{in}$ was measured in dendritic knobs of rat ORNs with a Cl^--sensitive fluorescent dye (Kaneko et al. 2004). E_{rev} is the reversal (zero current) potential through the channel or transporter. Because NKCC and KCC are electroneutral, their ionic fluxes do not depend on voltage. The stoichiometry of NCX was assumed to be $3Na^+/1Ca^{2+}$. The last column (fluxes) shows the predicted direction of ionic movements at an assumed neuronal resting potential of −75 mV.

both $[Na^+]_{in}$ and $[K^+]_{out}$ are unusually elevated. There is no single ion with an equilibrium potential as negative as the neuronal resting potential. Such apparent discrepancies may be misleading. Although the estimates shown in Table 1 are the best available, the free ionic concentrations across the ciliary membrane are still not known with high precision. It may also be that the resting potential in the cilium is determined in the cell body, where the ionic gradients are unknown. Alternatively, it may depend on an electrogenic, multi-ion transport system with a negative reversal potential.

In frog vomeronasal neurons, for example, activity of the Na^+,K^+-ATPase sets a negative resting potential (Trotier and Døving 1996). Table 1 also shows the predicted directions of ion fluxes through several relevant channels and transporters. Questions surrounding these predictions will be treated in subsequent sections.

With the exception of Cl^-, the mechanisms of ionic homeostasis at rest have not been studied. Cl^- is accumulated by ORNs (Table 1). A Na^+,K^+,$2Cl^-$ cotransporter (NKCC1) contributes substantially to Cl^- uptake at rest, but other as yet unidentified Cl^- transporters are also involved (Kaneko et al. 2004; Reisert et al. 2005; Nickell et al. 2006, 2007).

Many ORNs fire occasional APs in the apparent absence of stimulation (e.g., Gesteland et al. 1965; Trotier and MacLeod 1983; Ma et al. 1999; Duchamp-Viret et al. 2000; Tomaru and Kurahashi 2005). The membrane time constant is typically ~60 ms, so electrical events much faster than ~16 Hz are reduced in amplitude (Schild and Restrepo 1998). Because the phosphodiesterase inhibitor IBMX depolarizes ORNs, it is believed that both adenylyl cyclase and phosphodiesterase enzymes are active at rest.

The receptor current is carried by the ciliary CNG and Cl^- channels. The properties of these channels relevant to odor transduction will now be examined.

CNG channels

Nakamura and Gold (1987) discovered that the membrane of the olfactory cilium contains channels gated by cyclic nucleotides. Several lines of evidence showed that these channels are required for transduction of most odorants. Current through the channels was carried about equally by Na^+ or K^+, and this was also true of the odor-induced current in intact neurons (Kurahashi 1989). Stimulation with odorants and elevation of cyclic nucleotides activated channels with similar properties (Firestein, Zufall, Shepherd 1991). Most convincingly, knockout mice missing the CNG channel subunit CNGA2 lacked EOG responses to most odorants tested (Brunet et al. 1996). Since that initial report, residual responses to some odorants have been demonstrated in mice lacking CNGA2 (Zhao and Reed 2001; Lin et al. 2004).

Each CNG channel is a tetramer consisting of 2 CNGA2 subunits, 1 CNGA4 subunit, and 1 CNGB1b subunit (Bradley et al. 1994; Liman and Buck 1994; Sautter et al. 1998; Bönigk et al. 1999; Zheng and Zagotta 2004). The channels are present in almost all olfactory cilia examined (Kleene et al. 1994; Takeuchi and Kurahashi 2002). The soma and dendrite also express the channels but at much lower densities (Lowe and Gold 1993a; Kurahashi and Kaneko 1993). The channel density in the cilium has been estimated by several methods with widely differing results: 1750 channels/μm^2 in toad (Kurahashi and Kaneko 1993), 67–202 channels/μm^2 in frog (Kleene et al. 1994; Larsson et al. 1997), and 8 channels/μm^2 in rat (Reisert et al. 2003). With a given method, the density also varies widely from one cilium to the next (Kurahashi and Kaneko 1993; Kleene et al. 1994). Even the highest of these estimates is far below the geometric limit (~11 500 channels/μm^2 for a channel 10 nm in diameter with hexagonal close packing).

Properties of the native olfactory CNG channels have been determined in many vertebrates. (For a review of the older literature, see Table 2 of Schild and Restrepo [1998].) I will first describe the channel's properties in the absence of divalent cations. The unit conductance ranges from 8 to 46 pS (Zufall, Shepherd, and Firestein 1991; Frings et al. 1992; Zufall and Firestein 1993; Kurahashi and Kaneko 1993; Larsson et al. 1997). The channels are slightly more permeable to Na^+ than to K^+ (pK/pNa = 0.81–0.84 (Frings et al. 1992; Balasubramanian et al. 1996)), and the current-voltage relation shows slight outward rectification (Frings et al. 1992; Kurahashi and Kaneko 1993; Bönigk et al. 1999; Takeuchi and Kurahashi 2002). Like the neuronal response to odorants, the relation between concentration of cAMP and CNG current is well-fit by a Hill function. Half-maximal activation ($K_{½}$) occurs in various preparations from 2 to 37 (Figure 5, filled circles; Nakamura and Gold 1987; Frings et al. 1992; Kurahashi and Kaneko 1993; Kleene 1999; Bönigk et al. 1999). cGMP is a somewhat more effective ligand, gating half-maximally at 0.7–20 μM. The Hill slope

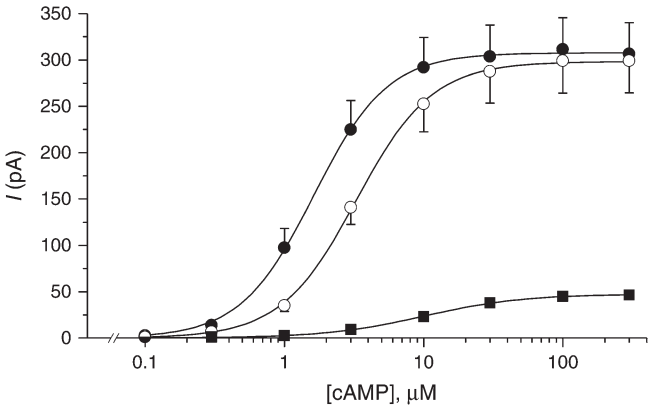

Figure 5 Effects of extracellular and cytoplasmic Ca^{2+} on the dose–response relation of the olfactory CNG channel. Current activated by various concentrations of cAMP at −50 mV was measured in single frog olfactory cilia. Filled circles: dose–response relation with $[Ca^{2+}]_{out}$ = 0 (nominally) and $[Ca^{2+}]_{in}$ = 0.1 μM (concentrations given are for free Ca^{2+}). The parameters of the best-fitting Hill function are I_{max} = 306 pA, $K_{½}$ = 1.7 μM, n = 1.7. Open circles: effect of increasing cytoplasmic Ca^{2+} ($[Ca^{2+}]_{out}$ = 0 and $[Ca^{2+}]_{in}$ = 3 μM). The dose–response relation is shifted to higher concentrations. The parameters of the best-fitting Hill function are I_{max} = 299 pA, $K_{½}$ = 3.4 μM, n = 1.6. Inhibition of current is greater at low [cAMP]. Compared to the first curve (filled circles, $[Ca^{2+}]_{in}$ = 0.1 μM), current activated by 1 μM cAMP has been reduced by 64%, whereas current activated by 10 μM cAMP has been reduced by just 13%. Filled squares: effect of increasing extracellular Ca^{2+} ($[Ca^{2+}]_{out}$ = 1 mM and $[Ca^{2+}]_{in}$ = 0.1 μM). The parameters of the best-fitting Hill function are I_{max} = 47 pA, $K_{½}$ = 10.3, n = 1.3. The dose–response relation is shifted to higher concentrations. Current is greatly reduced by open-channel block at every concentration of cAMP. Currents in this figure are inward but assigned positive values. Modified from Kleene (1999) with permission of the American Physiological Society.

parameter *n* ranges from 1.3 to 2.3. From this, it has long been imagined that at least 2 molecules of cAMP must bind before the channel will gate. Recently, it was shown that binding of the second cAMP molecule brings the channel almost to its maximum open probability (Nache et al. 2005; Biskup et al. 2007), which is just 0.7–0.8 (Kurahashi and Kaneko 1993; Larsson et al. 1997; Kleene 1997; Reisert et al. 2003). Once activated, the channel current does not spontaneously inactivate (Zufall, Firestein, and Shepherd 1991; Kramer and Siegelbaum 1992; Kurahashi and Kaneko 1993). Phosphatidylinositol 3,4,5-trisphosphate greatly decreases the sensitivity of the CNG channel to cAMP (Zhainazarov et al. 2004). Many reagents block current through these channels, but no specific inhibitor is known (reviewed by Brown et al. 2006).

CNG channels are modulated by divalent cations on either side of the ciliary membrane. Ca^{2+} and Mg^{2+} have profound effects, both direct and indirect, on the odor-induced receptor current. Modulation by extracellular divalent cations will be described first. It was found that part of the odor-induced current is due to an influx of Ca^{2+} (Kurahashi and Shibuya 1990), yet the current is much larger when extracellular Ca^{2+} is removed (Kurahashi 1989). In single CNG channels, Zufall and Firestein (1993) showed that entry of extracellular Ca^{2+} and Mg^{2+} at negative potentials produces an open-channel block. The open CNG channel conducts divalent cations but once in the channel they bind transiently. This temporary block reduces the current carried by all cations, leaving the single-channel conductance very small (~1.5 pS [Zufall and Firestein 1993]; 0.56 pS [Kleene 1997]). At positive potentials, the extracellular divalent cations are less driven to enter the channel, so the block is somewhat relieved. Near the resting potential and with a saturating concentration of cAMP, half-maximal effects were seen at 30 μM Ca^{2+} and 200 μM Mg^{2+} in salamander (Zufall and Firestein 1993); in a subsequent study in frog (Kleene 1995), these values were 180 μM for Ca^{2+} and 280 μM for Mg^{2+}. Extracellular Ca^{2+} reduces the CNG current much more effectively at lower cAMP concentrations (Figure 5, filled squares). This has the effect of making the CNG channels less sensitive to cAMP (Kleene 1999). A study of CNG channels in photoreceptors offers a possible mechanism. In those channels, the affinity between Ca^{2+} and the channel (i.e., open-channel block) decreases as the concentration of cyclic nucleotide increases (Hackos and Korenbrot 1999). With increasing levels of extracellular Ca^{2+}, a higher fraction of the current through the olfactory CNG channels is carried by Ca^{2+}. This has been demonstrated by exogenous coexpression of the 3 CNG channel subunits from rat. With 2 mM extracellular Ca^{2+}, the fraction of current carried by Ca^{2+} at –70 mV is 0.4 (Dzeja et al. 1999). It has not yet been possible to measure this value with the native channels.

The receptor current is also greatly influenced by intraciliary Ca^{2+}, which acts in concert with one or more Ca^{2+}-binding factors. It was found that cytoplasmic Ca^{2+} greatly reduces the open probability, but not the unit conductance, of the CNG channel (Zufall, Shepherd, and Firestein 1991). The shift was similar at both negative and positive potentials, making open-channel block an unlikely explanation. The effect of Ca^{2+} is gradually lost after isolation of a membrane patch, so it was suggested that a diffusible Ca^{2+}-binding factor was involved (Kramer and Siegelbaum 1992). Ultimately it was discovered that calmodulin (CaM) can function in this role (Chen and Yau 1994). To have a channel that is rapidly modulated by Ca^{2+}–CaM requires the presence of all 3 channel subunits (Munger et al. 2001; Bradley et al. 2001). Even with just 100 nM Ca^{2+}, CaM constitutively associates with exogenously expressed CNG channels (Bradley et al. 2004). As with open-channel block by extracellular Ca^{2+}, the effect of cytoplasmic Ca^{2+}–CaM is much greater at lower concentrations of cAMP (Kramer and Siegelbaum 1992; Lynch and Lindemann 1994). As before, the effect of this is to shift the dose–response relation to higher cAMP concentrations (Figure 5, open circles). In the native channel, as little as 2 μM Ca^{2+} produces a significant shift (Chen and Yau 1994). In rat, higher levels of Ca^{2+} increase the half-maximally effective concentration of cAMP by factors ranging from 3 to 20 (Lynch and Lindemann 1994; Chen and Yau 1994; Balasubramanian et al. 1996; Bradley et al. 2004). Although the dose–response relation is shifted, the maximal current at saturating [cAMP] is unchanged in rat by Ca^{2+} concentrations as high as 70 μM (Kramer and Siegelbaum 1992; Chen and Yau 1994). As discussed by Pifferi, Boccaccio, and Menini (2006), it is still not certain whether factors other than CaM may mediate the effects of cytoplasmic Ca^{2+} on the CNG channel in vivo.

One might have predicted that, like extracellular Ca^{2+}, cytoplasmic Ca^{2+} would directly reduce current through the CNG channels by open-channel block. When Ca^{2+}-binding factors are washed off the membrane, though, no effect of 300-μM cytoplasmic Ca^{2+} on the current is found at –50 or +50 mV (unpublished analysis of data from Kleene 1999). Thus, open-channel block by cytoplasmic Ca^{2+} may be negligible under physiological conditions. Cytoplasmic Mg^{2+} at physiological concentrations does produce a strong, voltage-dependent open-channel block (Kleene 1993a). Because the block is only effective at positive potentials, it probably has little effect on transduction.

In summary, cAMP activates cationic CNG channels in the ciliary membrane. Under physiological conditions, much of the inward current is carried by Ca^{2+}. Extracellular Ca^{2+} and Mg^{2+} reduce inward CNG current by open-channel block. Elevated cytoplasmic Ca^{2+}, together with one or more Ca^{2+}-binding factors such as CaM, reduces the sensitivity of the channels to cAMP.

Calcium-gated chloride channels

As shown in Figure 4, a second channel contributes to the olfactory receptor current. This is a Ca^{2+}-gated Cl^- channel

that has been described in ORNs of amphibia (Kleene and Gesteland 1991b; Kurahashi and Yau 1993), mammals (Lowe and Gold 1993b; Reisert et al. 2003), and fish (Sato and Suzuki 2000). In frog, the channels are present in virtually all the olfactory cilia (Kleene et al. 1994). The channel density in the cilium is estimated to be 62–78/μm^2 (Larsson et al. 1997; Reisert et al. 2003). In frog, the densities of the CNG and Cl^- channels are similar (Larsson et al. 1997). In rat, though, Cl^- channels are in excess by a factor of ~8 (Reisert et al. 2003).

The current conducted by a single olfactory Cl^- channel is so small that single-channel studies have not been possible. By noise analysis of macroscopic currents, the unit conductance was estimated to be just 0.8 pS in frog (Larsson et al. 1997). Low-pass filtering below 100 Hz reduces the measured conductance to 0.5 pS (Kleene 1997). In a neuron, which is expected to cut off frequencies below ~16 Hz (Schild and Restrepo 1998), it is likely that the effective conductance is smaller still. The unit conductance is ~1.5 pS in rat (Reisert et al. 2003) and 1.6 pS in mouse (Pifferi, Pascarella, et al. 2006). These values are similar to the unit conductance of the CNG channel in physiological solutions (~1.5 pS [Zufall and Firestein 1993]; 0.56 pS [Kleene 1997]). Not surprisingly, then, the ratio of maximum CNG and Cl^- currents in physiological solutions primarily reflects the relative abundances of the 2 types of channel. In frog, the maximum currents are almost equal (Kleene 1993b, 1997). In rat, where the Cl^- channels are more numerous, the maximum Cl^- current is greater than the maximum CNG current by a factor of 33 (Reisert et al. 2003).

The relation between $[Ca^{2+}]_{in}$ and Cl^- current is well-fit by a Hill function. Studies in frog (Kleene and Gesteland 1991b), rat (Reisert et al. 2003), and mouse (Reisert et al. 2005; Pifferi, Pascarella, et al. 2006) have shown that half-maximal activation ($K_{½}$) occurs from 2.2 to 4.7 μM Ca^{2+}. (In one other study, $K_{½}$ was much higher [26 μM; Hallani et al. 1998]; the reason for this difference is unknown.) Gating of the channel is probably cooperative; the Hill slope parameter n ranges from 2.0 to 2.8. The channel's maximum open probability is 0.97. The shape of the current-voltage relation varies with concentration of the gating ligand. At 2–3 μM Ca^{2+}, significant outward rectification is apparent. At saturating Ca^{2+} levels, though, inward rectification is seen (Kleene and Gesteland 1991b). In neither case is the mechanism of rectification known. One cannot yet exclude the possibility that 2 Cl^- channels, one with each type of rectification, contribute to the current.

The molecular identity of the olfactory Cl^- channel is unknown. Bestrophin-2 has been identified as a candidate (Pifferi, Pascarella, et al. 2006). However, knockout mice lacking bestrophin-2 showed no deficit in a simple behavioral assay of olfactory function (Bakall et al. 2008). It is not known whether ORNs from these mice have the olfactory Cl^- current or whether this current is required for normal olfactory behavior.

No modulators of the olfactory Cl^- channel are known. It is apparently not affected by CaM (Kleene 1999; Reisert et al. 2003) or Ca^{2+}–CaM–dependent protein kinase II (CaMKII; Kleene SJ, unpublished observations). In rat (Reisert et al. 2003) but not in frog (Kleene and Gesteland 1991b), the amplitude of the Cl^- current gradually decreases after excision of a membrane patch (Reisert et al. 2003). Whether this reflects loss of a diffusible channel modulator has not been determined. Pharmacological inhibitors of the olfactory Cl^- channel exist and have been reviewed elsewhere (Kleene 2002).

Generation of the receptor current

The channel properties just described permit a reasonably detailed explanation of the generation and termination of the receptor current. Successful binding of odorant molecules initiates a G-protein–coupled cascade that elevates intraciliary cAMP (Figure 4). cAMP gates the CNG channels, thus initiating the receptor current. As described above, there is a latency of up to 600 ms between the arrival of the stimulus and the onset of the receptor current. This is found even in isolated ORNs, where diffusion through the mucus is not a factor. As noted by Kurahashi et al. (1994), the cascade leading to production of cAMP is unlikely to be this slow. In fact, the latency may reflect a balance between 2 competing effects of the odorant: activation and suppression. Some (but not all) odorants suppress the response to other odorants (Gesteland et al. 1965; Kurahashi et al. 1994; Leinders-Zufall et al. 1997; Yamada and Nakatani 2001; Oka et al. 2004; Chen et al. 2006; Rospars et al. 2008). In exogenous expression systems, 2 mechanisms for this have been demonstrated. First, an odorant can have both agonistic and antagonistic effects on binding to the receptor (Leinders-Zufall et al. 1997; Araneda et al. 2000; Oka et al. 2004). Second, some odorants can directly inhibit the expressed CNG channels (Chen et al. 2006).

The production of cAMP in the cilia has been measured directly by Takeuchi and Kurahashi (2005) during prolonged odor stimulation. During the rising phase of the response, the rate of cAMP production was found to increase linearly with time. At most, all the neuronal cilia combined generated ~200 000 molecules of cAMP per second per cell. Given the high surface-to-volume ratio of the cilium, though, cAMP concentrations were as high as 129 μM, which was ~6 times the half-maximally effective concentration of cAMP ($K_{½}$).

CNG channels gated by the cAMP allow a significant influx of Ca^{2+}, and this is the source of the Ca^{2+} that gates the ciliary Cl^- channels (Kleene 1993b). Estimates of the intraciliary Ca^{2+} concentration in responding ORNs vary widely. Measurements with a Ca^{2+}-sensitive fluorescent dye suggest that $[Ca^{2+}]_{in}$ does not exceed 300 nM (Leinders-Zufall et al. 1998). However, Cl^- channels are gated during the odor response (Kurahashi and Yau 1993; Lowe and Gold 1993b; Zhainazarov and Ache 1995; Reisert and Matthews 1998). This implies that $[Ca^{2+}]_{in}$ reaches at least 2 μM, given the dose–response relation for the Cl^- channels. By using

a Ca^{2+}-gated K^+ channel as a sensor, it was concluded that $[Ca^{2+}]_{in}$ reaches at least 100 μM during the odor response (Delgado and Bacigalupo 2004). Fluorescence imaging of Ca^{2+} suggests that it is distributed nonuniformly within a responding cilium (Leinders-Zufall et al. 1998).

In most ORNs, Cl^- exits the cilium when the Cl^- channels are gated (Kurahashi and Yau 1993; Lowe and Gold 1993b; Zhainazarov and Ache 1995; Reisert and Matthews 1998; but see also Okada et al. 2000). This, together with the influx of cations through the CNG channels, causes the neuronal depolarization. The relative contributions of the 2 currents are species dependent. For a strong stimulus, the Cl^- current is 36–65% of the total current in amphibians (Kurahashi and Yau 1993; Lowe and Gold 1993b; Zhainazarov and Ache 1995) but 80–90% in rat (Reisert et al. 2003) and mouse (Nickell et al. 2006; Boccaccio and Menini 2007). The ratio of the 2 currents is expected to vary with stimulus strength. One would predict that a very small response would generate too little intraciliary Ca^{2+} to gate the Cl^- channels. To date, this prediction has not been tested. One can also guess at how the ratio varies with time during a single response. Desensitization of the CNG channel by Ca^{2+}–CaM and gating of the Cl^- channels both begin when $[Ca^{2+}]_{in}$ reaches ~2 μM. At that point, the current might switch from mostly cationic to mostly Cl^-.

For stimuli of weak to moderate strength, the dose–response relation to odorants (Figure 2B) often rises steeply. At least 4 elements of the transduction cascade contribute to this:

1. For both the CNG and Cl^- channels, the relation between ligand concentration and gating shows positive cooperativity (i.e., a Hill coefficient $n > 1$). Thus, for each channel type, there is a range over which the response increases quickly with increasing concentration of ligand.
2. As [cAMP] increases, the inhibitory effects of Ca^{2+}–CaM are reduced (Figure 5, open circles).
3. Open-channel block of the CNG channels by extracellular Ca^{2+} and Mg^{2+} also decreases as [cAMP] increases (Figure 5, filled squares).
4. In a neuron that is not voltage clamped, open-channel block will be further relieved by depolarization (Zufall and Firestein 1993).

Note that the steepness of the dose–response relation is entirely ascribed to properties of the CNG and Cl^- channels, and this has been verified experimentally (Takeuchi and Kurahashi 2002). The high surface-to-volume ratio of the cilium should render coupling between the 2 channel types very efficient. Were there no mechanisms for buffering or expulsion of Ca^{2+}, opening just 7 CNG channels for 1 s would bring $[Ca^{2+}]_{in}$ to 5 μM, which would be sufficient to gate half of the Cl^- channels. (This assumes a unitary CNG channel current of 28 fA [Kleene 1997] and an intraciliary volume of 0.2 fL [Lindemann 2001].)

The onset of the receptor current should also be influenced by any buffers of cAMP or Ca^{2+}. The channels themselves should act as buffers (Flannery et al. 2006; Takeuchi and Kurahashi 2008), and several Ca^{2+}-binding proteins have been identified at the mucosal surface, perhaps in the cilia (Boekhoff et al. 1997; Moon et al. 1998; Mammen et al. 2004; Uebi et al. 2007).

Termination of the receptor current

Even as the receptor current is generated, processes commence that inactivate it. These processes underlie adaptation and desensitization. There is abundant evidence that normal inactivation requires an influx of Ca^{2+}. The falling phase of the odor response is slowed or eliminated at positive potentials (Kurahashi and Shibuya 1990; Lowe and Gold 1993a; Takeuchi et al. 2003), in the absence of extracellular Ca^{2+} (Kurahashi and Shibuya 1990; Kurahashi 1990; Zufall, Shepherd, and Firestein 1991) or on addition of an intracellular Ca^{2+} chelator (Kurahashi and Shibuya 1990). Each of these conditions inhibits the accumulation of cytoplasmic free Ca^{2+}. Adaptation to repeated brief stimuli is also greatly reduced at positive potentials (Takeuchi and Kurahashi 2003; Boccaccio et al. 2006). Finally, the receptor current begins to decline just as the Ca^{2+} concentration peaks (Leinders-Zufall et al. 1998; Reisert and Matthews 2001c).

The current generated by photorelease of cAMP also shows Ca^{2+}-dependent adaptation (Kurahashi and Menini 1997). Thus, at least, part of the inactivation occurs at steps in the cascade following the activation of cyclase. However, the inactivation during a prolonged odor stimulus is faster than that seen during prolonged release of caged cAMP (Takeuchi and Kurahashi 2002). This indicates that other mechanisms of inactivation exist upstream of the channels. At least 10 mechanisms may contribute to termination of the receptor current. Six of these may contribute to termination of brief stimuli:

1. G_{olf} is inactivated by its intrinsic GTPase function.
2. cAMP and Ca^{2+} should diffuse away from the channels.
3. Phosphodiesterases hydrolyze cAMP. The ciliary phosphodiesterase PDE1C2 is activated by CaMKII (Borisy et al. 1992; Yan et al. 1995).
4. As described above, Ca^{2+} and Ca^{2+}-binding factors such as CaM make the CNG channels less sensitive to cAMP.
5. Ca^{2+} is expelled from the ciliary membrane by Na^+-dependent Ca^{2+} extrusion (as discussed below).
6. Ciliary Ca^{2+}-gated K^+ channels (Delgado et al. 2003; Delgado and Bacigalupo 2004) could help to repolarize the neuron, although the equilibrium potential for K^+ is apparently not very negative (Table 1).

Other mechanisms contribute to termination of responses to prolonged or intense stimulation:

1. G-protein–coupled receptor kinase 3 (GRK3) and β-arrestin-2 can inactivate the odorant receptor protein (Dawson et al. 1993; Schleicher et al. 1993; Peppel et al. 1997; Mashukova et al. 2006).
2. Ca^{2+}–CaM activates CaMKII, which in turn phosphorylates the type III adenylyl cyclase (Boekhoff et al. 1996; Wei et al. 1998; Leinders-Zufall et al. 1999). Early results (reviewed by Boekhoff et al. 1996) were complex, but it is now believed that this inhibits the cyclase, thus reducing the production of cAMP. The cyclase is also inhibited by RGS2, but the role of this in transduction is uncertain (Sinnarajah et al. 2001).
3. The suppressive effect of odorants described above may contribute.
4. Intraciliary Cl^- should be depleted during a prolonged response (Lindemann 2001), and this would limit or prevent further Cl^- efflux. Such depletion does not occur during brief stimulation (Boccaccio et al. 2006).

The relative importances of these mechanisms to termination and adaptation are not yet established. Evidence suggests that the 2 assays for adaptation described above do not reflect identical mechanisms (Song et al. 2008). Additional processes mediated by cGMP, carbon monoxide, and nitric oxide may also contribute to long-term adaptation. These have been reviewed elsewhere (Zufall and Leinders-Zufall 2000).

No processes have been identified that inactivate the Cl^- channels. When successive pulses of intraciliary Ca^{2+} are created by photolysis of caged Ca^{2+}, the Cl^- current does not decrease (Boccaccio et al. 2006).

Restoration of the resting ionic gradients

Response recovery includes reestablishment of the resting ionic gradients. Lindemann (2001) has modeled the ionic movements during a prolonged odor response. Such a response is predicted to have 3 effects on intraciliary ionic concentrations: an elevation of Ca^{2+} and depletions of Cl^- and K^+.

In the absence of a mechanism for expulsion of Ca^{2+}, intraciliary Ca^{2+} would reach millimolar levels (Lindemann 2001). There is evidence for 2 mechanisms of expulsion. The first mechanism is likely to be a Na^+/Ca^{2+} exchanger (NCX). Replacing extracellular Na^+ increases $[Ca^{2+}]_{in}$ at rest (Jung et al. 1994; Noé et al. 1997) and prolongs the odor-induced Cl^- current (Reisert and Matthews 1998, 2001a; Antolin and Matthews 2007; Castillo et al. 2007). There is no dependence on K^+ (Jung et al. 1994; Reisert et al. 2003), so an $Na^+/Ca^{2+}+K^+$ exchanger (NCKX) is unlikely to account for the activity. NCX typically has a low affinity for Ca^{2+} ($K_{½}$ > 1 μM) and a high transport capacity (Brini and Carafoli 2000), so it should be effective at reducing the high levels of cytoplasmic Ca^{2+} produced during a strong odor response.

A second method for expelling intraciliary Ca^{2+} is the plasma membrane calcium ATPase (PMCA). Several PMCA isoforms have been localized to the olfactory cilia (Weeraratne et al. 2006). Membrane fractions enriched in olfactory cilia have PMCA activity (Lo et al. 1994; Castillo et al. 2007) and express a novel PMCA-like protein (Klimmeck et al. 2008). Inhibiting PMCA prolongs the current activated by cAMP in ORNs (Castillo et al. 2007). In the presence of CaM, PMCA usually has a higher affinity for Ca^{2+} ($K_{½}$ < 0.5 μM) and a lower capacity (Brini and Carafoli 2000) than NCX.

As noted by Lindemann (2001), high NCX activity in its forward mode (3 Na^+ in, 1 Ca^{2+} out per cycle) would soon cause a large increase in intraciliary Na^+ and that in turn would limit Ca^{2+} efflux by NCX. Accumulation of Na^+ is likely to be reversed by a Na^+,K^+-ATPase. Such an ATPase has been identified in olfactory cilia by cytochemical (Kern et al. 1991; Menco et al. 1998), biochemical (Lo et al. 1991), and proteomic (Klimmeck et al. 2008; Mayer et al. 2008) methods.

The odor response is also predicted to deplete the cilium of K^+ and Cl^- (Lindemann 2001). In theory, those ions could be replenished by uptake through a K^+,Cl^- cotransporter (KCC). Some mouse ORNs do show intense dendritic labeling for KCC2 (Schannen and Delay 2005).

In general, the regulation and thermodynamics of ionic homeostasis in olfactory cilia are not clear. NCX, for example, is supposed to contribute to Ca^{2+} efflux as the odor response terminates. At rest, though, the ionic gradients (Table 1) should cause a Ca^{2+} *influx* at –75 mV. If only $[Ca^{2+}]_{in}$ were varied, it would need to exceed 4 mM before Ca^{2+} efflux could be supported. Depolarization would make Ca^{2+} expulsion by NCX even more difficult. The thermodynamic basis of Cl^- accumulation is also uncertain. At rest, NKCC is believed to contribute to Cl^- uptake, whereas the ionic gradients predict Cl^- extrusion. Equilibrium for NKCC has a second-order dependence on $[Cl^-]$, so small changes in $[Cl^-]$ can easily reverse the direction of transport. For example, reducing $[Cl^-]_{in}$ below 35 mM would cause accumulation of Cl^- to be favored.

Signal-to-noise issues

With what confidence can a given neuronal AP be attributed to the binding of an odorant? Confidence is increased if it is likely that odorant binding will generate activity greater than is typically encountered in the absence of odor.

This condition should be more easily met if the resting membrane current and potential are stable and below the threshold for generation of APs. Under voltage clamp, the resting current is indeed stable, with little fluctuation (Firestein and Werblin 1989; Kurahashi 1989; Lowe and Gold 1993b). Under current clamp, though, fast potential fluctuations of 1–3 mV have been observed, superimposed on larger fluctuations as large as 10 mV (Trotier 1986). In

unstimulated frog olfactory epithelium, the rate of AP firing is typically less than 20 per minute (Gesteland et al. 1965; Sicard and Holley 1984). In rat (Duchamp-Viret et al. 2000) or catfish (Kang and Caprio 1995), though, resting activity often exceeds 100 APs per min. Such high rates of spontaneous activity should make reliable detection of weak stimuli more difficult.

Confidence should also be increased if odorant binding generates a large depolarization. This is facilitated by amplifications in the transduction cascade, but only for stimuli above a certain concentration. Consider the Hill functions shown on linear axes in Figure 6. In a system with no cooperativity ($n = 1$), a very small stimulus may generate 2 μM cAMP and cause a detectable response. The slope of the dose–response relation is always decreasing, and so a much stronger stimulus (e.g., one producing 20 μM cAMP) only gives a moderately greater response. With positive cooperativity ($n = 5$), the slope of the relation increases up to an inflection point (9.2 μM in the example). The response to 20 μM cAMP is increased, but 3 μM cAMP may go undetected. Whether this is a useful trade-off is not obvious.

A better dose–response relation might combine the sensitivity of the first relation ($n = 1$) and the steepness of the second ($n = 5$). If the resting neuron were to maintain [cAMP] at 4 μM, for example, one could regard the dose–response relation as shifted to the left by that amount (the dashed curve in Figure 6, where [cAMP] now refers to the additional cAMP generated by transduction). The ORN may achieve this to a small extent. In the absence of stimuli, the ORN maintains a cytoplasmic cAMP concentration of 0.1–0.3 μM (Pun and Kleene 2003). This should set the transduction cascade somewhat closer to the start of the region of high slope.

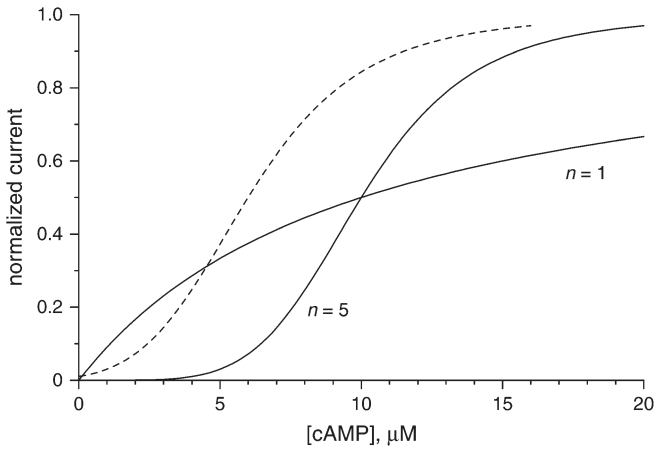

Figure 6 Predicted effects of positive cooperativity on the sensitivity and dynamic range of the odor response. The 2 solid curves are theoretical dose–response relations showing the receptor current as a function of [cAMP] in the cilium. Each curve is a Hill function with $K_{½}$ = 10 μM and $n = 1$ or $n = 5$. Increasing n decreases the response when [cAMP] is below $K_{½}$ (10 μM) but increases it when [cAMP] exceeds $K_{½}$. Increasing n also decreases the dynamic range. This can arbitrarily be defined in terms of the cAMP levels that give 10% and 90% of the maximal response. With $n = 1$, 10% and 90% occur at 1.1 and 90 μM; with $n = 5$, 10% and 90% occur at 6.4 and 15.5 μM. The ratios of the 90–10% values are 81 if $n = 1$ but just 2.4 if $n = 5$. The dashed curve is the equation with $n = 5$ shifted 4 μM to the left. See the text for additional details.

In summary, the steepness of the dose–response relation prevents responses at very low levels of cAMP but enhances responses at higher levels. As discussed by Lowe and Gold (1995), very low levels of cAMP might arise from spontaneous activity of transduction proteins. A highly cooperative dose–response relation would block responses from such noise, as well as responses from weak stimuli. As noted above, the steepness of the dose–response relation may be less prominent in ORNs with intact membranes.

Noise contributed by the receptor current itself is reduced by 2 factors. The current arises from the gating of large numbers of CNG and Cl^- channels. Under physiological conditions, each channel has a very small unitary current (25–28 fA). Having a large number of small channels reduces channel noise for a given mean current. In fact, the Cl^- channels amplify the receptor current with no significant increase in noise (Kleene 1997).

In addition, amplification by the Cl^- channels should produce a temporal filtering of fast channel noise. The current through each Cl^- channel reflects the local $[Ca^{2+}]_{in}$, which depends in part on the integral of the Ca^{2+} influx over a relatively long time. Ca^{2+} reaching a given Cl^- channel originates from several CNG channels, so a spatial averaging of noise should also occur (Reisert et al. 2003).

The lower limit of stimulus detection

It has long been wondered whether binding of a single odorant molecule to an ORN might produce a detectable electrical response. Odorants at minimally effective concentrations elicit small current "bumps" of 0.3–1 pA reminiscent of those sometimes produced by rod photoreceptors on absorption of a single photon. It was proposed that the current bumps produced by ORNs might result from binding of single odorant molecules (Menini et al. 1995). However, this interpretation was challenged because the current bumps do not sum linearly with stimulus dose as expected for a single-molecule response (Gold 1995). Subsequently, it was shown that photolysis of caged cAMP in the cilium causes similar current fluctuations even in the absence of odorants (Lowe and Gold 1995).

Bhandawat et al. (2005) reexamined the question under conditions in which the current amplitude is linearly related to stimulus dose. In a reduced Ca^{2+} bath, the amplitudes of neuronal responses to weak stimuli were found to be integral multiples of 0.9 pA (Bhandawat et al. 2005). This suggests that successful binding of a single molecule of odorant may produce a response of 0.9 pA. In physiological solutions, the event amplitude could only be inferred from noise analysis. The estimated amplitude was 26 fA (Bhandawat

et al. 2005). This is remarkably close to the unitary current of the CNG channel in physiological solutions (28 fA; Kleene 1997). The opening of one CNG channel is probably the smallest event that the noise analysis could have detected. It seems likely, then, that there is no amplification early in transduction. Binding of one odorant molecule leads to the gating of at most one CNG channel. Bhandawat et al. (2005) estimate that binding of the odorants tested is so brief (~1 ms) that receptor activation rarely results. Given an odorant with much higher affinity (Grosmaitre et al. 2006), binding might persist long enough to activate multiple G_{olf} molecules and provide an early amplification. The GTP exchange factor Ric-8b may also increase the probability of G_{olf} activation (Von Dannecker et al. 2005).

Whether binding of a single molecule of odorant could really be detected (i.e., could lead to an AP) has not been determined. In an intact rat ORN, a channel current of 1 pA was sufficient to cause an AP, provided that the duration of the opening was sufficient (Lynch and Barry 1989). Such a current should require the successful binding of several hundred odorant molecules. In whole-cell studies, injection of 1–3 pA of current is sufficient to trigger an AP (Firestein and Werblin 1987; Imanaka and Takeuchi 2001; Tomaru and Kurahashi 2005).

Conduction and integration of responses

The cilium's extreme geometry should influence the conduction and integration of electrical responses. In the frog, the cilium's length exceeds its diameter by a factor of ~100 (Reese 1965). Because of the cilium's small diameter, resistance to longitudinal current in the cytoplasm is significant. If this becomes comparable to the membrane resistance, the electrotonic length of the cilium decreases. The signal will then attenuate as it is conducted down the length of the cilium.

In an isolated, unstimulated frog cilium, the electrotonic length is 3–5 times the physical length of the cilium (Kleene 1992; Kleene et al. 1994). A signal traveling down such a fiber will experience little attenuation, and a moderate number of small, simultaneous local currents should add linearly. However, as more and more transduction channels are gated, the membrane resistance decreases, and the effect of each succeeding local depolarization is reduced. If all the CNG channels in a cilium are gated, the electrotonic length is only about 15% of the physical length (Kleene et al. 1994).

The spatial integration of multiple stimuli has been studied experimentally. With a Ca^{2+}-sensitive fluorescent dye (Leinders-Zufall et al. 1998) and with electrophysiology (Takeuchi and Kurahashi 2008), it has been shown that the individual cilia on a given neuron are equivalent and operate as independent functional units. As expected, a pair of small stimuli on a given cilium adds simply, whereas larger stimuli add sublinearly (Takeuchi and Kurahashi 2008).

Another source of nonadditivity could be overlapping transduction domains. Second messengers would be expected to diffuse from one domain to other domains nearby. However, 2 small stimuli created 2 μm apart on a single cilium were found to add simply. This suggests that diffusion of second messengers is inconsequential at distances >2 μm, at least during small responses (Takeuchi and Kurahashi 2008).

Spatial distributions of the proteins serving transduction

The cilia function to increase the neuronal surface area by a factor of ~40 (Menco 1997), increasing the probability of odorant binding. One might expect that the transduction proteins would be uniformly expressed along the ciliary membrane.

Ultrastructural studies by Menco and his colleagues found that this is often not the case. The CNGA2 channel subunit, G_{olf}, and the type III adenylyl cyclase are much more heavily expressed in the distal segment of the cilium than in the proximal part (Menco et al. 1992; Matsuzaki et al. 1999). (In rat, the proximal segment is 2–3 μm long and 0.3 μm in diameter; the distal segment is 50–60 μm long and 0.1 μm in diameter [Menco 1980; Matsuzaki et al. 1999].) GRK3, β-arrestin-2, PDE1C2, and CaMKII were found in both ciliary segments (Menco 2005), as were 2 putative odorant receptors (Menco et al. 1997). Another odorant receptor appears to be uniformly expressed along the ciliary length (Schwarzenbacher et al. 2005).

More recently, functional assays have also shown that the distribution of the CNG channels along the cilium is nonuniform. In frog cilia ranging from 25 to 100 μm in length, the channels are usually heavily expressed in a band near the start of the distal segment, and often some are found near the base of the cilium. Between these regions, and in the more distal portions, channel expression is low (Flannery et al. 2006). In newt ORNs, channel density near the base of the 12-μm cilia could not be determined. Channels were found along the remaining length, with density again decreasing in the more distal parts (Takeuchi and Kurahashi 2008). The low CNG channel expression near the base of the cilium is notable. In *Chlamydomonas*, deflagellation results if $[Ca^{2+}]_{in}$ reaches ~1 μM at the distal end of the transition zone (Lohret et al. 1998; Quarmby 2004). A lack of CNG channels in that region of the olfactory cilium might prevent Ca^{2+} accumulation and deciliation.

The proximity of individual CNG and Cl^- channels is of particular interest. If each CNG channel were a sufficient distance from the nearest Cl^- channel, then the incoming Ca^{2+} could be consumed by buffers or transporters before reaching the Cl^- channel. Thus, proximity should enhance amplification. By modeling the effect of a buffer while recording the cationic and Cl^- currents, it was concluded that the 2 channel types are only as close as would be predicted by uniform distributions (Reisert et al. 2003).

It is unclear to what extent ionic homeostasis is a function of the cilium. In one study, NKCC1 was found in the

proximal dendrite and soma but not in the dendritic knob or cilia (Reisert et al. 2005). In a second study, moderate ciliary immunoreactivity for NKCC was found (Menco 2005). A functional study suggested that NKCC activity was located apically in the epithelium (Kaneko et al. 2004). Proteomic analyses have not detected NKCC in olfactory cilia (Klimmeck et al. 2008; Mayer et al. 2008).

Na^+/Ca^{2+} exchange occurs in the cilium and, perhaps, other apical compartments. An early physiological study localized exchange to the neuronal dendrite or cilia (Jung et al. 1994). Subsequently, Reisert and Matthews (1998) found that bathing just the cilia in an Na^+-free solution was sufficient to prolong the odor-induced Cl^- current. Na^+/Ca^{2+} exchange has been demonstrated in membrane preparations enriched in olfactory cilia (Castillo et al. 2007). NCX1 is preferentially expressed in the apical part of the ORN (Pyrski et al. 2007). However, it is also expressed in immature ORNs that lack cilia (Pyrski et al. 2007). Surprisingly, NCX is not evident in proteomic analyses of the cilia (Klimmeck et al. 2008; Mayer et al. 2008). Evidence cited above also suggests that PMCA and Na^+,K^+-ATPase function in the cilia.

It seems likely that, to some extent, the cilium may rely on the dendrite or soma for ionic homeostasis. To what extent the ciliary basal body might restrict diffusion is unknown. Lucifer yellow (molecular weight 450 Da) can pass from the soma into the cilia (Takeuchi and Kurahashi 2008), whereas green fluorescent protein (molecular weight 26.9 kDa) cannot (Elsaesser and Paysan 2007). Whether this diffusion barrier hinders small ions is unknown.

Balance of functional trade-offs

Depending on its function, a sensory neuron may be imagined to benefit from optimizing speed of transduction, stimulus specificity, sensitivity, and/or dynamic range.

Clearly, the ORN is not optimized for speed. The response latency is often several hundred milliseconds, although this depends on the species and the experimental protocol. The duration of the response to odors can be several seconds. We do not require a lightning fast reflex triggered by smell.

A fundamental and unusual property of the olfactory system is its very broad stimulus specificity, allowing it to detect and discriminate among thousands of distinct odorants. Not surprisingly, then, single ORNs studied also have fairly broad stimulus specificities. Each ORN responds to a variety of odorants, and each odorant can activate several different receptor proteins (Gesteland, Lettivin, et al. 1965; Sicard and Holley 1984; Malnic et al. 1999; Duchamp-Viret et al. 2000; Kajiya et al. 2001; Touhara 2002). Processing at the olfactory bulb and beyond probably accounts for the ability to discriminate more odorants than there are receptor proteins. Having ORNs with overlapping sensitivities should enhance olfactory discrimination at the bulb (Sánchez-Montañés and Pearce 2002). Stimulus coding has recently been reviewed (Touhara 2002, 2007; Malnic 2007).

This broad specificity may in part account for the limited sensitivity of ORNs. ORNs typically respond to odorants at concentrations of 1–100 μM. By contrast, vomeronasal neurons of the mouse respond to pheromones at concentrations as low as 10 pM (Leinders-Zufall et al. 2000). The lower sensitivity of the olfactory system likely results from the receptor proteins. Each receptor can bind many ligands, but this probably requires that most of the binding affinities be low. Because of this, an odorant molecule typically binds for just 1 ms, and most odorant–receptor interactions fail to activate a receptor (Bhandawat et al. 2005). The later stages of transduction do ensure that a successful binding event results in a detectable current.

Does olfactory transduction benefit from using a cascade of CNG and Cl^- channels? This is a difficult question. With strong stimulation, it is clear that the Cl^- channels greatly amplify the receptor current. However, the rate of AP firing saturates at lower concentrations than does the receptor current (Reisert and Matthews 1999; Tomaru and Kurahashi 2005), so Cl^- amplification becomes inconsequential before the channels are saturated with Ca^{2+}. At the other extreme, very weak stimuli may never elevate $[Ca^{2+}]_{in}$ enough to gate any Cl^- channels. Above some moderately low stimulus level (which has not been determined), addition of a Cl^- current probably does increase the rate of AP firing. It is interesting to consider alternative designs. In the laboratory, one can easily arrange for a very large receptor current with no Cl^- component. In amphibians (Kurahashi 1989) and mouse (Reisert et al. 2005; Boccaccio et al. 2006), the CNG channels alone can produce the largest receptor current if block by extracellular divalent cations is relieved. (Not surprisingly, chelation of Ca^{2+} in the mucus has been used to treat hyposmia (Panagiotopoulos et al. 2005).) However, such a system would lack the adaptation that results from a Ca^{2+} influx. One can also imagine a system where every Cl^- channel is replaced by a CNG channel. If several CNG channels were clustered near each molecule of adenylyl cyclase, this simpler design might still allow the normal current amplitude as well as adaptation. Involvement of the Cl^- channels should increase cooperativity, and perhaps, this improves the signal-to-noise properties. The Ca^{2+}-activated Cl^- efflux may simply have evolved to allow depolarization in fresh water, where monovalent cations are scarce (Kurahashi and Yau 1993; Kurahashi and Yau 1994; Kleene and Pun 1996).

The dynamic range of a given ORN may cover a 10-fold or a 1000-fold range of odorant concentration. For the whole organism, the dynamic range for a given odorant probably arises from several populations of ORNs, each with a different receptor protein sensitive to that odorant. For a given ORN, the dynamic range can be extended through adaptation during prolonged stimulation. The use of low-conductance channels ensures that the response is finely graded to stimulus strength across the dynamic range. As noted by Trotier (1994), such gradation would fail were a high-resistance neuron to use large transduction channels.

What we do not know

For the principal mechanism of vertebrate olfactory transduction, many molecular components and some important modulators have been identified. The molecular identities of the Ca^{2+}-gated Cl^- channel and the protein underlying Na^+-dependent Ca^{2+} extrusion are unknown. It is also unclear whether Ca^{2+}-binding proteins other than CaM may mediate desensitization of the CNG channels and what Ca^{2+} buffers may regulate $[Ca^{2+}]_{in}$. The type III adenylyl cyclase (Bakalyar and Reed 1990) and the CNGA2 subunit of the CNG channel (Bönigk et al. 1999) are glycosylated, but the functions of these glycosylations are not known. Analyses of the ciliary proteome (Mayer et al. 2008) and transcriptome (McClintock et al. 2008) may identify new ciliary proteins involved in transduction.

We are far from having a quantitative understanding of the transduction process. Computational frameworks are being developed (e.g., Lindemann 2001; Suzuki et al. 2004; Dougherty et al. 2005; Reidl et al. 2006; Rospars et al. 2008), but many key parameters have no experimental support. Even the resting state of the cilium is not well understood. Is diffusion within the cilium limited by the axoneme, which may occlude much of the ciliary volume (Lindemann 2001)? Does the basal body hinder diffusion between the cilium and the dendritic knob, and does this influence ionic homeostasis? The thermodynamic basis of ciliary ionic homeostasis is mysterious. It is not clear whether the cilium's resting ionic gradients are controlled at the cilium or in the dendrite and soma. Undiscovered factors in the cytoplasm or the mucus may influence the dynamic range. This might explain why, in all species examined, the dose–response relation is much shallower if the neuronal membrane is intact.

Binding affinities and catalytic rates for most of the transduction proteins have never been measured. (We can estimate some of them by analogy with other systems.) We do not know the balance between the cationic and Cl^- currents as a function of stimulus strength or as a function of time during any response. One can still wonder if the 2-channel system has an advantage that has escaped our attention.

The speed and efficiency of transduction will certainly depend on the physical locations of the proteins involved. How are the receptor proteins, G_{olf}, and type III adenylyl cyclase distributed along the ciliary length? For the CNG channels, low-resolution density distributions are becoming available. Are the Cl^- channels similarly distributed? We should ask the same questions at an even finer level. Evidence suggests that some ciliary transduction proteins are distributed in microdomains such as lipid rafts (Schreiber et al. 2000; Goldstein et al. 2003; Brady et al. 2004; Saavedra et al. 2008). Is each CNG channel right next to a Cl^- channel, thus allowing a fast and efficient amplification? The evidence to date suggests that the answer is "no" (Reisert et al. 2003).

It is trivial to pose these questions but not to answer them. It should be remembered, though, that 20 years ago, almost nothing in this review was known.

Funding

National Science Foundation (DMS-0515989); University Research Council of the University of Cincinnati.

Acknowledgements

I am grateful to Nancy Kleene and the 3 anonymous reviewers for many corrections and improvements to the manuscript and to Glenn Doerman for creating Figure 1A.

References

Ache BW, Young JM. 2005. Olfaction: Diverse species, conserved principles. Neuron. 48:417–430.

Adamek GD, Gesteland RC, Mair RG, Oakley B. 1984. Transduction physiology of olfactory receptor cilia. Brain Res. 310:87–97.

Anderson PAV, Hamilton KA. 1987. Intracellular recordings from isolated salamander olfactory receptor neurons. Neuroscience. 21:167–173.

Antolin S, Matthews HR. 2007. The effect of external sodium concentration on sodium-calcium exchange in frog olfactory receptor cells. J Physiol. 581:495–503.

Araneda RC, Kini AD, Firestein S. 2000. The molecular receptive range of an odorant receptor. Nat Neurosci. 3:1248–1255.

Bakall B, McLaughlin P, Stanton JB, Zhang Y, Hartzell HC, Marmorstein LY, Marmorstein AD. 2008. Bestrophin-2 is involved in the generation of intraocular pressure. Invest Ophthalmol Vis Sci. 49:1563–1570.

Bakalyar HA, Reed RR. 1990. Identification of a specialized adenylyl cyclase that may mediate odorant detection. Science. 250:1403–1406.

Balasubramanian S, Lynch JW, Barry PH. 1996. Calcium-dependent modulation of the agonist affinity of the mammalian olfactory cyclic nucleotide-gated channel by calmodulin and a novel endogenous factor. J Membr Biol. 152:13–23.

Bhandawat V, Reisert J, Yau K-W. 2005. Elementary response of olfactory receptor neurons to odorants. Science. 308:1931–1934.

Biskup C, Kusch J, Schulz E, Nache V, Schwede F, Lehmann F, Hagen V, Benndorf K. 2007. Relating ligand binding to activation gating in CNGA2 channels. Nature. 446:440–443.

Boccaccio A, Lagostena L, Hagen V, Menini A. 2006. Fast adaptation in mouse olfactory sensory neurons does not require the activity of phosphodiesterase. J Gen Physiol. 128:171–184.

Boccaccio A, Menini A. 2007. Temporal development of cyclic nucleotide-gated and Ca^{2+}-activated Cl^- currents in isolated mouse olfactory sensory neurons. J Neurophysiol. 98:153–160.

Boekhoff I, Braunewell KH, Andreini I, Breer H, Gundelfinger E. 1997. The calcium-binding protein VILIP in olfactory neurons: regulation of second messenger signaling. Eur J Cell Biol. 72:151–158.

Boekhoff I, Kroner C, Breer H. 1996. Calcium controls second-messenger signalling in olfactory cilia. Cell Signal. 8:167–171.

Bönigk W, Bradley J, Müller F, Sesti F, Boekhoff I, Ronnett GV, Kaupp UB, Frings S. 1999. The native rat olfactory cyclic nucleotide-gated channel is composed of three distinct subunits. J Neurosci. 19:5332–5347.

Borisy FF, Ronnett GV, Cunningham AM, Juilfs D, Beavo J, Snyder SH. 1992. Calcium/calmodulin-activated phosphodiesterase expressed in olfactory receptor neurons. J Neurosci. 12:915–923.

Bradley J, Bönigk W, Yau K-W, Frings S. 2004. Calmodulin permanently associates with rat olfactory CNG channels under native conditions. Nat Neurosci. 7:705–710.

Bradley J, Li J, Davidson N, Lester HA, Zinn K. 1994. Heteromeric olfactory cyclic nucleotide-gated channels: A subunit that confers increased sensitivity to cAMP. Proc Natl Acad Sci USA. 91:8890–8894.

Bradley J, Reisert J, Frings S. 2005. Regulation of cyclic nucleotide-gated channels. Curr Opin Neurobiol. 15:343–349.

Bradley J, Reuter D, Frings S. 2001. Facilitation of calmodulin-mediated odor adaptation by cAMP-gated channel subunits. Science. 294:2176–2178.

Brady JD, Rich TC, Le X, Stafford K, Fowler CJ, Lynch L, Karpen JW, Brown RL, Martens JR. 2004. Functional role of lipid raft microdomains in cyclic nucleotide-gated channel activation. Mol Pharmacol. 65:503–511.

Brini M, Carafoli E. 2000. Calcium signalling: a historical account, recent developments and future perspectives. Cell Mol Life Sci. 57:354–370.

Brown RL, Strassmaier T, Brady JD, Karpen JW. 2006. The pharmacology of cyclic nucleotide-gated channels: Emerging from the darkness. Curr Pharm Des. 12:3597–3613.

Brunet LJ, Gold GH, Ngai J. 1996. General anosmia caused by a targeted disruption of the mouse olfactory cyclic nucleotide-gated cation channel. Neuron. 17:681–693.

Buck L, Axel R. 1991. A novel multigene family may encode odorant receptors: a molecular basis for odor recognition. Cell. 65:175–187.

Castillo K, Delgado R, Bacigalupo J. 2007. Plasma membrane Ca^{2+}-ATPase in the cilia of olfactory receptor neurons: possible role in Ca^{2+} clearance. Eur J Neurosci. 26:2524–2531.

Chen S, Lane AP, Bock R, Leinders-Zufall T, Zufall F. 2000. Blocking adenylyl cyclase inhibits olfactory generator currents induced by "IP_3-odors". J Neurophysiol. 84:575–580.

Chen T-Y, Takeuchi H, Kurahashi T. 2006. Odorant inhibition of the olfactory cyclic nucleotide-gated channel with a native molecular assembly. J Gen Physiol. 128:365–371.

Chen T-Y, Yau K-W. 1994. Direct modulation by Ca^{2+}-calmodulin of cyclic nucleotide-activated channel of rat olfactory receptor neurons. Nature. 368:545–548.

Chiu P, Lynch JW, Barry PH. 1997. Odorant-induced currents in intact patches from rat olfactory receptor neurons: Theory and experiment. Biophys J. 72:1442–1457.

Crumling MA, Gold GH. 1998. Ion concentrations in the mucus covering the olfactory epithelium in rodents. Soc Neurosci Abstr. 24:2099.

Dawson TM, Arriza JL, Jaworsky DE, Borisy FF, Attramadal H, Lefkowitz RJ, Ronnett GV. 1993. β-adrenergic receptor kinase-2 and β-arrestin-2 as mediators of odorant-induced desensitization. Science. 259:825–829.

Delgado R, Bacigalupo J. 2004. Cilium-attached and excised patch-clamp recordings of odourant-activated Ca-dependent K channels from chemosensory cilia of olfactory receptor neurons. Eur J Neurosci. 20: 2975–2980.

Delgado R, Saavedra MV, Schmachtenberg O, Sierralta J, Bacigalupo J. 2003. Presence of Ca^{2+}-dependent K^+ channels in chemosensory cilia support a role in odor transduction. J Neurophysiol. 90:2022–2028.

Dhallan R, Yau K-W, Schrader KA, Reed RR. 1990. Primary structure and functional expression of a cyclic nucleotide-activated channel from olfactory neurons. Nature. 347:184–187.

Dougherty DP, Wright GA, Yew AC. 2005. Computational model of the cAMP-mediated sensory response and calcium-dependent adaptation in vertebrate olfactory receptor neurons. Proc Natl Acad Sci USA. 102: 10415–10420.

Duchamp-Viret P, Duchamp A, Chaput MA. 2000. Peripheral odor coding in the rat and frog: Quality and intensity specification. J Neurosci. 20: 2383–2390.

Dzeja C, Hagen V, Kaupp UB, Frings S. 1999. Ca^{2+} permeation in cyclic nucleotide-gated channels. EMBO J. 18:131–144.

Elsaesser R, Paysan J. 2007. The sense of smell, its signalling pathways, and the dichotomy of cilia and microvilli in olfactory sensory sells. BMC Neurosci. 8(Suppl 3):S1.

Firestein S. 2001. How the olfactory system makes sense of scents. Nature. 413:211–218.

Firestein S, Darrow B, Shepherd GM. 1991. Activation of the sensory current in salamander olfactory receptor neurons depends on a G protein-mediated cAMP second messenger system. Neuron. 6:825–835.

Firestein S, Picco C, Menini A. 1993. The relation between stimulus and response in olfactory receptor cells of the tiger salamander. J Physiol. 468:1–10.

Firestein S, Shepherd GM, Werblin FS. 1990. Time course of the membrane current underlying sensory transduction in salamander olfactory receptor neurones. J Physiol. 430:135–158.

Firestein S, Werblin F. 1987. Gated currents in isolated olfactory receptor neurons of the larval tiger salamander. Proc Natl Acad Sci USA. 84: 6292–6296.

Firestein S, Werblin F. 1989. Odor-induced membrane currents in vertebrate-olfactory receptor neurons. Science. 244:79–82.

Firestein S, Zufall F, Shepherd GM. 1991. Single odor-sensitive channels in olfactory receptor neurons are also gated by cyclic nucleotides. J Neurosci. 11:3565–3572.

Flannery RJ, French DA, Kleene SJ. 2006. Clustering of cyclic-nucleotide-gated channels in olfactory cilia. Biophys J. 91:179–188.

Frings S, Lindemann B. 1988. Odorant response of isolated olfactory receptor cells is blocked by amiloride. J Membr Biol. 105:233–243.

Frings S, Lindemann B. 1990. Single unit recording from olfactory cilia. Biophys J. 57:1091–1094.

Frings S, Lindemann B. 1991. Current recording from sensory cilia of olfactory receptor cells in situ. I. The neuronal response to cyclic nucleotides. J Gen Physiol. 97:1–16.

Frings S, Lynch JW, Lindemann B. 1992. Properties of cyclic nucleotide-gated channels mediating olfactory transduction. J Gen Physiol. 100:45–67.

Gesteland RC, Lettvin JY, Pitts WH, Rojas A. 1963. Odor specificities of the frog's olfactory receptors. In: Zotterman Y, editor. Olfaction and Taste. New York: Pergamon Press. pp.19–34.

Gesteland RC, Lettvin JY, Pitts WH. 1965. Chemical transmission in the nose of the frog. J Physiol. 181:525–559.

Getchell TV. 1977. Analysis of intracellular recordings from salamander olfactory epithelium. Brain Res. 123:275–286.

Getchell TV. 1986. Functional properties of vertebrate olfactory receptor neurons. Physiol Rev. 66:772–818.

Gold GH. 1995. Single odorant molecules? Nature. 376:27.

Goldstein BJ, Kulaga HM, Reed RR. 2003. Cloning and characterization of SLP3: a novel member of the stomatin family expressed by olfactory receptor neurons. J Assoc Res Otolaryngol. 4:74–82.

Grosmaitre X, Vassalli A, Mombaerts P, Shepherd GM, Ma M. 2006. Odorant responses of olfactory sensory neurons expressing the odorant receptor MOR23: a patch clamp analysis in gene-targeted mice. Proc Natl Acad Sci USA. 103:1970–1975.

Hackos DH, Korenbrot JI. 1999. Divalent cation selectivity is a function of gating in native and recombinant cyclic nucleotide-gated ion channels from retinal photoreceptors. J Gen Physiol. 113:799–817.

Hallani M, Lynch JW, Barry PH. 1998. Characterization of calcium-activated chloride channels in patches excised from the dendritic knob of mammalian olfactory receptor neurons. J Membr Biol. 161:163–171.

Hirono J, Sato T, Tonoike M, Takebayashi M. 1992. Simultaneous recording of $[Ca^{2+}]_i$ increases in isolated olfactory receptor neurons retaining their original spatial relationship in intact tissue. J Neurosci Methods. 42: 185–194.

Hopkins AE. 1926. The olfactory receptors in vertebrates. J Comp Neurol. 41:253–289.

Imanaka Y, Takeuchi H. 2001. Spiking properties of olfactory receptor cells in the slice preparation. Chem Senses. 26:1023–1027.

Jones DT, Reed RR. 1989. G_{olf}: an olfactory neuron specific-G protein involved in odorant signal transduction. Science. 244:790–795.

Jung A, Lischka FW, Engel J, Schild D. 1994. Sodium/calcium exchanger in olfactory receptor neurones of *Xenopus laevis*. NeuroReport. 5: 1741–1744.

Kajiya K, Inaki K, Tanaka M, Haga T, Kataoka H, Touhara K. 2001. Molecular bases of odor discrimination: Reconstitution of olfactory receptors that recognize overlapping sets of odorants. J Neurosci. 21:6018–6025.

Kaneko H, Putzier I, Frings S, Kaupp UB, Gensch T. 2004. Chloride accumulation in mammalian olfactory sensory neurons. J Neurosci. 24: 7931–7938.

Kang J, Caprio J. 1995. In vivo responses of single olfactory receptor neurons in the channel catfish, *Ictalurus punctatus*. J Neurophysiol. 73:172–177.

Kaupp UB, Seifert R. 2002. Cyclic nucleotide-gated ion channels. Physiol Rev. 82:769–824.

Kawai F, Kurahashi T, Kaneko A. 1996. T-type Ca^{2+} channel lowers the threshold of spike generation in the newt olfactory receptor cell. J Gen Physiol. 108:525–535.

Kern RC, Kerr TP, Getchell TV. 1991. Ultrastructural localization of Na^+/K^+-ATPase in rodent olfactory epithelium. Brain Res. 546:8–17.

Kleene SJ. 1992. Basal conductance of frog olfactory cilia. Pflügers Arch. 421:374–380.

Kleene SJ. 1993a. The cyclic nucleotide-activated conductance in olfactory cilia: Effects of cytoplasmic Mg^{2+} and Ca^{2+}. J Membr Biol. 131:237–243.

Kleene SJ. 1993b. Origin of the chloride current in olfactory transduction. Neuron. 11:123–132.

Kleene SJ. 1995. Block by external calcium and magnesium of the cyclic-nucleotide-activated current in olfactory cilia. Neuroscience. 66: 1001–1008.

Kleene SJ. 1997. High-gain, low-noise amplification in olfactory transduction. Biophys J. 73:1110–1117.

Kleene SJ. 1999. Both external and internal calcium reduce the sensitivity of the olfactory cyclic-nucleotide-gated channel to cAMP. J Neurophysiol. 81:2675–2682.

Kleene SJ. 2000. Spontaneous gating of olfactory cyclic-nucleotide-gated channels. J Membr Biol. 178:49–54.

Kleene SJ. 2002. The calcium-activated chloride conductance in olfactory receptor neurons. Curr Topics Membr. 53:119–134.

Kleene SJ, Gesteland RC. 1981. Dissociation of frog olfactory epithelium with N-ethylmaleimide. Brain Res. 229:536–540.

Kleene SJ, Gesteland RC. 1991a. Transmembrane currents in frog olfactory cilia. J Membr Biol. 120:75–81.

Kleene SJ, Gesteland RC. 1991b. Calcium-activated chloride conductance in frog olfactory cilia. J Neurosci. 11:3624–3629.

Kleene SJ, Gesteland RC, Bryant SH. 1994. An electrophysiological survey of frog olfactory cilia. J Exp Biol. 195:307–328.

Kleene SJ, Pun RYK. 1996. Persistence of the olfactory receptor current in a wide variety of extracellular environments. J Neurophysiol. 75: 1386–1391.

Klimmeck D, Mayer U, Ungerer N, Warnken U, Schnölzer M, Frings S, Möhrlen F. 2008. Calcium-signaling networks in olfactory receptor neurons. Neuroscience. 151:901–912.

Kramer RH, Siegelbaum SA. 1992. Intracellular Ca^{2+} regulates the sensitivity of cyclic nucleotide-gated channels in olfactory receptor neurons. Neuron. 9:897–906.

Kurahashi T. 1989. Activation by odorants of cation-selective conductance in the olfactory receptor cell isolated from the newt. J Physiol. 419: 177–192; erratum in J Physiol. 2000 424:561–562.

Kurahashi T. 1990. The response induced by intracellular cyclic AMP in isolated olfactory receptor cells of the newt. J Physiol. 430:355–371.

Kurahashi T, Kaneko A. 1993. Gating properties of the cAMP-gated channels in toad olfactory receptor cells. J Physiol. 466:287–302.

Kurahashi T, Lowe G, Gold GH. 1994. Suppression of odorant responses by odorants in olfactory receptor cells. Science. 265:118–120.

Kurahashi T, Menini A. 1997. Mechanism of odorant adaptation in the olfactory receptor cell. Nature. 385:725–729.

Kurahashi T, Shibuya T. 1990. Ca^{2+}-dependent adaptive properties in the solitary olfactory receptor cell of the newt. Brain Res. 515:261–268.

Kurahashi T, Yau K-W. 1993. Co-existence of cationic and chloride components in odorant-induced current of vertebrate olfactory receptor cells. Nature. 363:71–74.

Kurahashi T, Yau K-W. 1994. Tale of an unusual chloride current. Curr Biol. 4:256–258.

Lagostena L, Menini A. 2003. Whole-cell recordings and photolysis of caged compounds in olfactory sensory neurons isolated from the mouse. Chem Senses. 28:705–716.

Larsson HP, Kleene SJ, Lecar H. 1997. Noise analysis of ion channels in non-space-clamped cables: Estimates of channel parameters in olfactory cilia. Biophys J. 72:1193–1203.

Leinders-Zufall T, Greer CA, Shepherd GM, Zufall F. 1998. Imaging odor-induced calcium transients in single olfactory cilia: Specificity of activation and role in transduction. J Neurosci. 18:5630–5639.

Leinders-Zufall T, Lane AP, Puche AC, Ma W, Novotny MV, Shipley MT, Zufall F. 2000. Ultrasensitive pheromone detection by mammalian vomeronasal neurons. Nature. 405:792–796; erratum in Nature. 2000 408:616.

Leinders-Zufall T, Ma M, Zufall F. 1999. Impaired odor adaptation in olfactory receptor neurons after inhibition of Ca^{2+}/calmodulin kinase II. J Neurosci. 19:RC19.

Leinders-Zufall T, Rand MN, Shepherd GM, Greer CA, Zufall F. 1997. Calcium entry through cyclic nucleotide-gated channels in individual cilia

of olfactory receptor cells: Spatiotemporal dynamics. J Neurosci. 17: 4136–4148.

Lidow MS, Menco BPhM. 1984. Observations on axonemes and membranes of olfactory and respiratory cilia in frogs and rats using tannic acid-supplemented fixation and photographic rotation. J Ultrastruct Res. 86: 18–30.

Liman ER, Buck LB. 1994. A second subunit of the olfactory cyclic nucleotide-gated channel confers high sensitivity to cAMP. Neuron. 13:611–621.

Lin W, Arellano J, Slotnick B, Restrepo D. 2004. Odors detected by mice deficient in cyclic nucleotide-gated channel subunit A2 stimulate the main olfactory system. J Neurosci. 24:3703–3710.

Lindemann B. 2001. Predicted profiles of ion concentrations in olfactory cilia in the steady state. Biophys J. 80:1712–1721.

Lo YH, Bradley TM, Rhoads DE. 1991. L-alanine binding sites and Na^+, K^+-ATPase in cilia and other membrane fractions from olfactory rosettes of Atlantic salmon. Comp Biochem Physiol B. 98:121–126.

Lo YH, Bradley TM, Rhoads DE. 1994. High-affinity Ca^{2+},Mg^{2+}-ATPase in plasma membrane-rich preparations from olfactory epithelium of Atlantic salmon. Biochim Biophys Acta. 1192:153–158.

Lohret TA, McNally FJ, Quarmby LM. 1998. A role for katanin-mediated axonemal severing during *Chlamydomonas* deflagellation. Mol Biol Cell. 9:1195–1207.

Lowe G, Gold GH. 1991. The spatial distributions of odorant sensitivity and odorant-induced currents in salamander olfactory receptor cells. J Physiol. 442:147–168.

Lowe G, Gold GH. 1993a. Contribution of the ciliary cyclic nucleotide-gated conductance to olfactory transduction in the salamander. J Physiol. 462:175–196.

Lowe G, Gold GH. 1993b. Nonlinear amplification by calcium-dependent chloride channels in olfactory receptor cells. Nature. 366:283–286.

Lowe G, Gold GH. 1995. Olfactory transduction is intrinsically noisy. Proc Natl Acad Sci USA. 92:7864–7868; erratum in Proc Natl Acad Sci USA. 1995 92:10817.

Lynch JW, Barry PH. 1989. Action potentials initiated by single channels opening in a small neuron (rat olfactory receptor). Biophys J. 55: 755–768.

Lynch JW, Barry PH. 1991. Properties of transient K^+ currents and underlying single K^+ channels in rat olfactory receptor neurons. J Gen Physiol. 97: 1043–1072.

Lynch JW, Lindemann B. 1994. Cyclic nucleotide-gated channels of rat olfactory receptor cells: Divalent cations control the sensitivity to cAMP. J Gen Physiol. 103:87–106.

Ma M. 2007. Encoding olfactory signals via multiple chemosensory systems. Crit Rev Biochem Mol Biol. 42:463–480.

Ma M, Chen WR, Shepherd GM. 1999. Electrophysiological characterization of rat and mouse olfactory receptor neurons from an intact epithelial preparation. J Neurosci Methods. 92:31–40.

Malnic B. 2007. Searching for the ligands of odorant receptors. Mol Neurobiol. 35:175–181.

Malnic B, Hirono J, Sato T, Buck LB. 1999. Combinatorial receptor codes for odors. Cell. 96:713–723.

Mammen A, Simpson JP, Nighorn A, Imanishi Y, Palczewski K, Ronnett GV, Moon C. 2004. Hippocalcin in the olfactory epithelium: a mediator of second messenger signaling. Biochem Biophys Res Commun. 322: 1131–1139; erratum in Biochem Biophys Res Commun. 2005 326: following 694.

Mashukova A, Spehr M, Hatt H, Neuhaus EM. 2006. β-arrestin2-mediated internalization of mammalian odorant receptors. J Neurosci. 26: 9902–9912.

Matsuzaki O, Bakin RE, Cai X, Menco BPM, Ronnett GV. 1999. Localization of the olfactory cyclic nucleotide-gated channel subunit 1 in normal, embryonic and regenerating olfactory epithelium. Neuroscience. 94: 131–140.

Matthews HR, Reisert J. 2003. Calcium, the two-faced messenger of olfactory transduction and adaptation. Curr Opin Neurobiol. 13:469–475.

Maue RA, Dionne VE. 1987. Patch-clamp studies of isolated mouse olfactory receptor neurons. J Gen Physiol. 90:95–125.

Mayer U, Ungerer N, Klimmeck D, Warnken U, Schnölzer M, Frings S, Möhrlen F. 2008. Proteomic analysis of a membrane preparation from rat olfactory sensory cilia. Chem Senses. 33:145–162.

McClintock TS, Glasser CE, Bose SC, Bergman DA. 2008. Tissue expression patterns identify mouse cilia genes. Physiol Genomics. 32:198–206.

Menco BPhM. 1980. Qualitative and quantitative freeze-fracture studies of olfactory and nasal respiratory structures of frog, ox, rat, and dog. I. A general survey. Cell Tissue Res. 207:183–209.

Menco BPhM. 1997. Ultrastructural aspects of olfactory signaling. Chem Senses. 22:295–311.

Menco BPhM. 2005. The fine-structural distribution of G-protein receptor kinase 3, β-arrestin-2, Ca^{2+}/calmodulin-dependent protein kinase II and phosphodiesterase PDE1C2, and a Cl^--cotransporter in rodent olfactory epithelia. J Neurocytol. 34:11–36.

Menco BPhM, Birrell GB, Fuller CM, Ezeh PI, Keeton DA, Benos DJ. 1998. Ultrastructural localization of amiloride-sensitive sodium channels and Na^+,K^+-ATPase in the rat's olfactory epithelial surface. Chem Senses. 23:137–149.

Menco BPM, Bruch RC, Dau B, Danho W. 1992. Ultrastructural localization of olfactory transduction components: the G protein subunit $G_{olf\alpha}$ and type III adenylyl cyclase. Neuron. 8:441–453.

Menco BPhM, Cunningham AM, Qasba P, Levy N, Reed RR. 1997. Putative odour receptors localize in cilia of olfactory receptor cells in rat and mouse: a freeze-substitution ultrastructural study. J Neurocytol. 26: 691–706.

Menco BPhM, Farbman AI. 1992. Ultrastructural evidence for multiple mucous domains in frog olfactory epithelium. Cell Tissue Res. 270:47–56.

Menco BPhM, Morrison EE. 2003. Morphology of the mammalian olfactory epithelium: Form, fine structure, function, and pathology. In: Doty RL, editor. Handbook of olfaction and gustation. 2nd edition. New York: Marcel Dekker. p. 17–49.

Menini A, Picco C, Firestein S. 1995. Quantal-like current fluctuations induced by odorants in olfactory receptor cells. Nature. 373:435–437.

Moon C, Jaberi P, Otto-Bruc A, Baehr W, Palczewski K, Ronnett GV. 1998. Calcium-sensitive particulate guanylyl cyclase as a modulator of cAMP in olfactory receptor neurons. J Neurosci. 18:3195–3205.

Mori K, Takahashi YK, Igarashi KM, Yamaguchi M. 2006. Maps of odorant molecular features in the mammalian olfactory bulb. Physiol Rev. 86: 409–433.

Munger SD, Lane AP, Zhong H, Leinders-Zufall T, Yau K-W, Zufall F, Reed RR. 2001. Central role of the CNGA4 channel subunit in Ca^{2+}-calmodulin-dependent odor adaptation. Science. 294:2172–2175.

Nache V, Schulz E, Zimmer T, Kusch J, Biskup C, Koopmann R, Hagen V, Benndorf K. 2005. Activation of olfactory-type cyclic nucleotide-gated channels is highly cooperative. J Physiol. 569:91–102.

Nakamura T, Gold GH. 1987. A cyclic nucleotide-gated conductance in olfactory receptor cilia. Nature. 325:442–444.

Nickell WT, Kleene NK, Gesteland RC, Kleene SJ. 2006. Neuronal chloride accumulation in olfactory epithelium of mice lacking NKCC1. J Neurophysiol. 95:2003–2006.

Nickell WT, Kleene NK, Kleene SJ. 2007. Mechanisms of neuronal chloride accumulation in intact mouse olfactory epithelium. J Physiol. 583: 1005–1020.

Noé J, Tareilus E, Boekhoff I, Breer H. 1997. Sodium/calcium exchanger in rat olfactory neurons. Neurochem Int. 30:523–531.

Oka Y, Omura M, Kataoka H, Touhara K. 2004. Olfactory receptor antagonism between odorants. EMBO J. 23:120–126.

Okada Y, Fujiyama R, Miyamoto T, Sato T. 2000. Comparison of a Ca^{2+}-gated conductance and a second-messenger-gated conductance in rat olfactory neurons. J Exp Biol. 203:567–573.

Omura M, Sekine H, Shimizu T, Kataoka H, Touhara K. 2003. *In situ* Ca^{2+} imaging of odor responses in a coronal olfactory epithelium slice. NeuroReport. 14:1123–1127; erratum in NeuroReport. 2003 14:1653.

Ottoson D. 1956. Analysis of the electrical activity of the olfactory epithelium. Acta Physiol Scand. 35(Suppl 122):1–83.

Pace U, Hanski E, Salomon Y, Lancet D. 1985. Odorant-sensitive adenylate cyclase may mediate olfactory reception. Nature. 316:255–258.

Panagiotopoulos G, Naxakis S, Papavasiliou A, Filipakis K, Papatheodorou G, Goumas P. 2005. Decreasing nasal mucus Ca^{++} improves hyposmia. Rhinology. 43:130–134.

Peppel K, Boekhoff I, McDonald P, Breer H, Caron MG, Lefkowitz RJ. 1997. G protein-coupled receptor kinase 3 (GRK3) gene disruption leads to loss of odorant receptor desensitization. J Biol Chem. 272:25425–25428.

Pifferi S, Boccaccio A, Menini A. 2006. Cyclic nucleotide-gated ion channels in sensory transduction. FEBS Lett. 580:2853–2859.

Pifferi S, Pascarella G, Boccaccio A, Mazzatenta A, Gustincich S, Menini A, Zucchelli S. 2006. Bestrophin-2 is a candidate calcium-activated chloride channel involved in olfactory transduction. Proc Natl Acad Sci USA. 103:12929–12934.

Pun RYK, Kleene SJ. 2003. Contribution of cyclic-nucleotide-gated channels to the resting conductance of olfactory receptor neurons. Biophys J. 84:3425–3435.

Pun RYK, Kleene SJ. 2004. An estimate of the resting membrane resistance of frog olfactory receptor neurones. J Physiol. 559:535–542.

Pyrski M, Koo JH, Polumuri SK, Ruknudin AM, Margolis JW, Schulze DH, Margolis FL. 2007. Sodium/calcium exchanger expression in the mouse and rat olfactory systems. J Comp Neurol. 501:944–958.

Quarmby LM. 2004. Cellular deflagellation. Int Rev Cytol. 233:47–91.

Rawson NE, Yee KK. 2006. Transduction and coding. Adv Otorhinolaryngol. 63:23–43.

Reese TS. 1965. Olfactory cilia in the frog. J Cell Biol. 25:209–230.

Reidl J, Borowski P, Sensse A, Starke J, Zapotocky M, Eiswirth M. 2006. Model of calcium oscillations due to negative feedback in olfactory cilia. Biophys J. 90:1147–1155.

Reisert J, Bauer PJ, Yau K-W, Frings S. 2003. The Ca-activated Cl channel and its control in rat olfactory receptor neurons. J Gen Physiol. 122:349–363.

Reisert J, Lai J, Yau K-W, Bradley J. 2005. Mechanism of the excitatory Cl^- response in mouse olfactory receptor neurons. Neuron. 45: 553–561.

Reisert J, Matthews HR. 1998. Na^+-dependent Ca^{2+} extrusion governs response recovery in frog olfactory receptor cells. J Gen Physiol. 112: 529–535.

Reisert J, Matthews HR. 1999. Adaptation of the odour-induced response in frog olfactory receptor cells. J Physiol. 519:801–813.

Reisert J, Matthews HR. 2001a. Response properties of isolated mouse olfactory receptor cells. J Physiol. 530:113–122.

Reisert J, Matthews HR. 2001b. Responses to prolonged odour stimulation in frog olfactory receptor cells. J Physiol. 534:179–191.

Reisert J, Matthews HR. 2001c. Simultaneous recording of receptor current and intraciliary Ca^{2+} concentration in salamander olfactory receptor cells. J Physiol. 535:637–645.

Reisert J, Yau K-W, Margolis FL. 2007. Olfactory marker protein modulates the cAMP kinetics of the odour-induced response in cilia of mouse olfactory receptor neurons. J Physiol. 585:731–740.

Restrepo D, Miyamoto T, Bryant BP, Teeter JH. 1990. Odor stimuli trigger influx of calcium into olfactory neurons of the channel catfish. Science. 249:1166–1168.

Reuter D, Zierold K, Schröder WH, Frings S. 1998. A depolarizing chloride current contributes to chemoelectrical transduction in olfactory sensory neurons *in situ*. J Neurosci. 18:6623–6630.

Rospars JP, Lansky P, Chaput M, Duchamp-Viret P. 2008. Competitive and noncompetitive odorant interactions in the early neural coding of odorant mixtures. J Neurosci. 28:2659–2666.

Saavedra MV, Smalla KH, Thomas U, Sandoval S, Olavarria K, Castillo K, Delgado MG, Delgado R, Gundelfinger ED, Bacigalupo J. et al., 2008. Scaffolding proteins in highly purified rat olfactory cilia membranes. NeuroReport. 19:1123–1126.

Sánchez-Montañés MA, Pearce TC. 2002. Why do olfactory neurons have unspecific receptive fields? BioSystems. 67:229–238.

Sato K, Suzuki N. 2000. The contribution of a Ca^{2+}-activated Cl^- conductance to amino-acid-induced inward current responses of ciliated olfactory neurons of the rainbow trout. J Exp Biol. 203:253–262.

Sautter A, Zong X, Hofmann F, Biel M. 1998. An isoform of the rod photoreceptor cyclic nucleotide-gated channel β subunit expressed in olfactory neurons. Proc Natl Acad Sci USA. 95:4696–4701.

Schannen AP, Delay R. 2005. Expression of Cl^- cotransporters in mouse olfactory neurons [Abstract]. Chem Senses. 30:A80; Available from: http://chemse.oxfordjournals.org/cgi/reprint/30/3/A1.

Schild D, Restrepo D. 1998. Transduction mechanisms in vertebrate olfactory receptor cells. Physiol Rev. 78:429–466.

Schleicher S, Boekhoff I, Arriza J, Lefkowitz RJ, Breer H. 1993. A β-adrenergic receptor kinase-like enzyme is involved in olfactory signal termination. Proc Natl Acad Sci USA. 90:1420–1424.

Schreiber S, Fleischer J, Breer H, Boekhoff I. 2000. A possible role for caveolin as a signaling organizer in olfactory sensory membranes. J Biol Chem. 275:24115–24123; erratum in J Biol Chem. 2004 279:1575.

Schwarzenbacher K, Fleischer J, Breer H. 2005. Formation and maturation of olfactory cilia monitored by odorant receptor-specific antibodies. Histochem Cell Biol. 123:419–428.

Scott JW, Scott-Johnson PE. 2002. The electroolfactogram: a review of its history and uses. Microsc Res Tech. 58:152–160.

Sicard G, Holley A. 1984. Receptor cell responses to odorants: similarities and differences among odorants. Brain Res. 292:283–296.

Sinnarajah S, Dessauer CW, Srikumar D, Chen J, Yuen J, Yilma S, Dennis JC, Morrison EE, Vodyanoy V, Kehrl JH. 2001. RGS2 regulates signal transduction in olfactory neurons by attenuating activation of adenylyl cyclase III. Nature. 409:1051–1055.

Song Y, Cygnar KD, Sagdullaev B, Valley M, Hirsh S, Stephan A, Reisert J, Zhao H. 2008. Olfactory CNG channel desensitization by Ca^{2+}/CaM via the B1b subunit affects response termination but not sensitivity to recurring stimulation. Neuron. 58:374–386.

Suzuki N, Takahata M, Shoji T, Suzuki Y. 2004. Characterization of electro-olfactogram oscillations and their computational reconstruction. Chem Senses. 29:411–424.

Takeuchi H, Imanaka Y, Hirono J, Kurahashi T. 2003. Cross-adaptation between olfactory responses induced by two subgroups of odorant molecules. J Gen Physiol. 122:255–264.

Takeuchi H, Kurahashi T. 2002. Photolysis of caged cyclic AMP in the ciliary cytoplasm of the newt olfactory receptor cell. J Physiol. 541:825–833.

Takeuchi H, Kurahashi T. 2003. Identification of second messenger mediating signal transduction in the olfactory receptor cell. J Gen Physiol. 122:557–567.

Takeuchi H, Kurahashi T. 2005. Mechanism of signal amplification in the olfactory sensory cilia. J Neurosci. 25:11084–11091.

Takeuchi H, Kurahashi T. 2008. Distribution, amplification, and summation of cyclic nucleotide sensitivities within single olfactory sensory cilia. J Neurosci. 28:766–775.

Tomaru A, Kurahashi T. 2005. Mechanisms determining the dynamic range of the bullfrog olfactory receptor cell. J Neurophysiol. 93:1880–1888.

Touhara K. 2002. Odor discrimination by G protein-coupled olfactory receptors. Microsc Res Tech. 58:135–141.

Touhara K. 2007. Deorphanizing vertebrate olfactory receptors: Recent advances in odorant-response assays. Neurochem Int. 51:132–139.

Trotier D. 1986. A patch-clamp analysis of membrane currents in salamander olfactory receptor cells. Pflügers Arch. 407:589–595.

Trotier D. 1994. Intensity coding in olfactory receptor cells. Semin Cell Biol. 5:47–54.

Trotier D, Døving KB. 1996. Direct influence of the sodium pump on the membrane potential of vomeronasal chemoreceptor neurones in frog. J Physiol. 490:611–621.

Trotier D, MacLeod P. 1983. Intracellular recordings from salamander olfactory receptor cells. Brain Res. 268:225–237.

Uebi T, Miwa N, Kawamura S. 2007. Comprehensive interaction of dicalcin with annexins in frog olfactory and respiratory cilia. FEBS J. 274: 4863–4876.

Von Dannecker LE, Mercadante AF, Malnic B. 2005. Ric-8B, an olfactory putative GTP exchange factor, amplifies signal transduction through the olfactory-specific G-protein Gαolf. J Neurosci. 25: 3793–3800.

Weeraratne SD, Valentine M, Cusick M, Delay R, Van Houten JL. 2006. Plasma membrane calcium pumps in mouse olfactory sensory neurons. Chem Senses. 31:725–730.

Wei J, Zhao AZ, Chan GCK, Baker LP, Impey S, Beavo JA, Storm DR. 1998. Phosphorylation and inhibition of olfactory adenylyl cyclase by CaM kinase II in neurons: a mechanism for attenuation of olfactory signals. Neuron. 21:495–504.

Yamada H, Nakatani K. 2001. Odorant-induced hyperpolarization and suppression of cAMP-activated current in newt olfactory receptor neurons. Chem Senses. 26:25–34.

Yan C, Zhao AZ, Bentley JK, Loughney K, Ferguson K, Beavo JA. 1995. Molecular cloning and characterization of a calmodulin-dependent phosphodiesterase enriched in olfactory sensory neurons. Proc Natl Acad Sci USA. 92:9677–9681.

Zhainazarov AB, Ache BW. 1995. Odor-induced currents in *Xenopus* olfactory receptor cells measured with perforated-patch recording. J Neurophysiol. 74:479–483.

Zhainazarov AB, Spehr M, Wetzel CH, Hatt H, Ache BW. 2004. Modulation of the olfactory CNG channel by Ptdlns(3,4,5)P_3. J Membr Biol. 201: 51–57.

Zhao H, Ivic L, Otaki JM, Hashimoto M, Mikoshiba K, Firestein S. 1998. Functional expression of a mammalian odorant receptor. Science. 279: 237–242.

Zhao H, Reed RR. 2001. X inactivation of the OCNC1 channel gene reveals a role for activity-dependent competition in the olfactory system. Cell. 104:651–660.

Zheng J, Zagotta WN. 2004. Stoichiometry and assembly of olfactory cyclic nucleotide-gated channels. Neuron. 42:411–421.

Zufall F, Firestein S. 1993. Divalent cations block the cyclic nucleotide-gated channel of olfactory receptor neurons. J Neurophysiol. 69: 1758–1768.

Zufall F, Firestein S, Shepherd GM. 1991. Analysis of single cyclic nucleotide-gated channels in olfactory receptor cells. J Neurosci. 11: 3573–3580.

Zufall F, Leinders-Zufall T. 2000. The cellular and molecular basis of odor adaptation. Chem Senses. 25:473–481.

Zufall F, Shepherd GM, Firestein S. 1991. Inhibition of the olfactory cyclic nucleotide gated ion channel by intracellular calcium. Proc Biol Sci. 246:225–230.

Accepted July 15, 2008